University of Stavanger

Faculty of Science and Technology

MASTER'S THESIS

Study program/ Specialization:	Spring semester, 2017
Petroleum Technology	
Drilling Engineering	Restricted access
Writer: Haavard Simonsen	………………………………………
	(Writer's signature)

Faculty supervisor: Jan Aage Aasen
External supervisor: Vibjørn Dagestad

Thesis title: An Introduction to the Welltec Annual Barrier and its Interaction with the Open Hole Formation

Credits (ECTS): 30

Key words:	Pages: 61
- Open hole packer - Annular barrier - Shrink pressure - Rock mechanics	
	+ enclosure: 6
	Stavanger, 15.06.2017
	Date/year

Front page for master thesis

Faculty of Science and
Technology

Abstract

Developments in drilling have opened for the construction of extended reach wells. They can have large intermediate and reservoir sections, which may need zonal isolation. To isolate the different zones, Welltec has developed an expandable metal packer, called the Welltec Annular Barrier (WAB).

The WAB can be placed inside either a preceding casing or against an open-hole formation. As the WAB is expanded into the formation, a shrink pressure will arise between the wellbore and the WAB. This will lead to a volumetric expansion of the borehole, and eventually fracture of the formation, if the pressure is large enough.

In this thesis, a comparison of the expansion of the WAB is made to a process known as autofrettage. In this process, two cylinders of different sizes are fitted together to create a stronger composite cylinder, which is caused by a shrink pressure between them and residual stresses. An equation for the shrink pressure is developed through the use of well-known equations and relations from mechanics of materials.

A model is developed where the sum of the radial deformations is used as input. It will return the resulting shrink pressure, and WAB and wellbore deformations. The maximum allowable shrink pressure and deformation sum is also presented, if formation properties are defined. The results can be used to determine if any damage will occur to the wellbore

The further the WAB expands into the formation, a higher setting pressure is created, as well as increased sealing potential. Modelling showed it has good potential to create high contact stresses. Design changes are proposed to optimize the functionality of the tool.

Qualifying placement of the WAB in an open-hole to NORSOK D-010 barrier requirement standards could help operators mitigate difficult challenges during drilling and completion, as well as reduce both capital expenditure and operational expense.

Acknowledgement

I would like to thank Welltec for giving me the opportunity to write this thesis. A special thanks goes out to Vibjørn Dagestad and Satish Kumar, who have shown great patience and provided guidance whenever needed.

The same goes for my supervisor, Jan Aage Aasen, who has always been positive. Without his help, I would not have been able to write this thesis.

Finally, I want to thank close family and classmates. Studying all these years would have been a dull experience without you.

Contents

List of Figures

Abbreviations

CAPEX	Capital expenditure
ECD	Equivalent circulating density
ECP	External casing packer
HPHT	High pressure, high temperature
ISO	International Organization for Standardization
NCS	Norwegian continental shelf
NORSOK	Norsk sokkels kokurranseposisjon
OPEX	Operational expenses
P&A (PP&A)	Plug and abandonment (permanent)
SCP	Sustained casing pressure
WAB	Welltec Annular Barrier
WAB LH	WAB as liner hanger
WAB WI	WAB for well integrity
WAB ZI	WAB for zonal isolation
WCS	Well Screens
WDM	Welltec Data Monitor
WDR	Welltec Data Receiver
WFV	Welltec Flow Valve
WMIT	Welltec Multi-set Injection Tool

Nomenclature

A	Cross-sectional area (m^2)
a	Inner radius of cylinder (m)
b	Outer radius of cylinder (m)
c_{final}	Common radius of inner and outer cylinder (m)
c_i	Outer radius of inner cylinder (m)
c_o	Inner radius of outer cylinder (m)
d	Depth (m or ft.)
E	Young's modulus (Pa)
F	Force (N)
g	Acceleration due to gravity (m/s^2 or 32.175 ft/s)
h	Vertical thickness (ft.)
K	Formation bulk modulus (Pa)
L	Length (m or ft.)
L'	Deformed length (m or ft.)
$\varnothing$	Porosity
p	Pressure (Pa or psi)
p_1	Internal pressure (Pa)
p_2	External pressure (Pa)
p_f	Fluid column pressure (Pa)
p_o	Overpressure (Pa)
p_p	Pore pressure (Pa or psi)
p_{pn}	Normal pore pressure (Pa)
p_s	Shrink pressure (Pa)
$p_{s,frac}$	Shrink pressure at fracture (Pa)
$p_{s,max}$	Maximum shrink pressure (Pa)
p_w	Well pressure (Pa)
p_{wf}	Well fracture pressure (Pa)
r	Radius (m or ft.)
T	Temperature (ºC)
t	Thickness (m)
u	Radial displacement (m)
u_i	Radial displacement of inner cylinder (m)
u_o	Radial displacement of outer cylinder (m)
v	Poisson's ratio
α	Coefficient of linear thermal expansion (ºC^{-1})
β	Biot's constant
γ	Formation specific gravity (s.g.)

γ_b	Rock formation specific weight (lbf/ft^3)
γ_w	Specific weight of water (lbf/ft^3)
ε	Strain
ε_r	Radial strain
ε_z	Axial strain
ε_θ	Tangential strain
P	Density (kg/m^3)
ρ_b	Formation bulk density (kg/m^3 or lbf/ft^3)
ρ_f	Fluid density (kg/m^3)
ρ_{pf}	Pore fluid density (kg/m^3)
ρ_r	Rock grain density (kg/m^3)
σ	Stress (Pa)
σ'	Effective stress (Pa)
σ_h	Minimum horizontal stress (Pa)
σ_H	Maximum horizontal stress (Pa)
σ_r	Radial stress (Pa)
σ'_r	Effective radial stress (Pa)
σ_v	Overburden (vertical) stress (Pa)
σ_z	Axial stress (Pa)
σ_θ	Tangential stress (Pa)
σ'_θ	Effective tangential stress (Pa)
τ	Shear stress (Pa)

1. Introduction

1.1 Background

Over the past years, major advancements have been achieved in regards to drilling and construction of wells. This has opened for extended reach wells with long intermediate and reservoir sections, often with demanding conditions. Isolation of influx zones above the reservoir or of different reservoir zones might be necessary. This has typically been done with cement, but a high-quality cement job can often be challenging to carry out.

Non-satisfactory sealing ability can lead to pressure communication to surface in one or more of the annuli. This is not in compliance to NORSOK D-010 requirements, and necessary mitigation operations can cause considerate expenses.

As a potential solution to this issue, Welltec has developed a multipurpose annular barrier, the Welltec Annular Barrier (WAB), that can be used to aid in assuring a proper cement job and create a high quality annular seal. As of the publication date of this thesis, it has been qualified to be placed inside a cased hole, but this requires good cement behind the casing. More qualifications are being done to take the WAB one step further, to see if it can function as a stand-alone barrier in the open-hole formation.

The WAB is a metal packer with elastomer sealing elements, which is expanded by applying pressure from surface through the base pipe. As it expands into the formation, a shrink pressure is created between the wall of the WAB and the formation. Due to this, a contact stress is created which seals off the annulus. However, if the resulting shrink pressure is too large, fracturing of the formation will occur.

Compared to older, more traditional solutions and technologies, the WAB can open for significant savings in both capital expenditure (CAPEX) and operational expenses (OPEX), which should be more relevant than ever, considering the major efforts that are being done in the petroleum industry to cut costs and increase effectivity.

An equation for the shrink pressure that arises between the WAB and the formation is developed by using well known relations and equations from mechanics of materials, such as Lamé equations for a thick-walled cylinder, strain-displacement relations, and stress-strain-temperature relations.

A model is developed, where the sum of the radial deformations is used as input. It returns the shrink pressure that is created, as well as the deformations of the WAB and the wellbore. Rock mechanics is used to calculate the maximum allowable shrink pressure and the maximum sum of the deformations.

Results show that high pressures and contact stresses are created at small deformations. Still, some changes can be made to the design of the WAB to take full advantage of its potential.

Some assumptions are made to simplify the problem, such as rock isotropy and ignoring temperature effects, but the results should give a good indication of the real-life situation.

1.2   Objectives

There are two main objectives in this thesis:

1. Give the reader an understanding of the WAB
   The WAB can serve several purposes during the drilling and completion of a well. After reading this thesis, the reader will hopefully be able to understand the functionality of the WAB and how it has the potential to solve various issues during the life of a well.

2. Model the interaction between the WAB and the formation
   The main goal of the WAB is to be able to function as a barrier against the open hole formation. It is therefore necessary to create a model which can imply if expansion of the WAB causes any damage to the surrounding formation.

1.3   Structure of the Thesis

The thesis is divided into two main parts, one discussing relevant theory and one with examples illustrating the differences between various formations and the impact of WAB and formation properties.

An in-depth description of the WAB and its uses is given in chapter 2. A couple of cases where it has been used are also presented.

In chapter 3, basic theory is covered briefly to help the reader understand the underlying mechanisms of the work that is done.

Chapter 4 covers theory and introduces equations regarding thick-walled cylinders. The equation for the shrink pressure is also presented here.

Rock mechanics relevant to the thesis is covered on chapter 5.

Various cases are given in chapters 5 and 6 to give a picture of how the WAB will interact with different formations and how a variation in rock and WAB properties will affect the results.

Discussion of the results and conclusions are given in the final two chapters, respectively.

2. Welltec Annular Barrier

In this chapter, a thorough introduction of the WAB is given. Included in the text is its functionality, design, qualifications, comparisons to conventional packers and a couple of field cases.

2.1 Design and Functionality

The Welltec Annular Barrier is a full bore, hydraulically expandable metal packer, combined with elastomer elements. It was first introduced in 2011 in the Valemon field project where there were several challenges caused by high pressure and high temperature wells. At the time, there were no good solutions available to meet these challenges, but three showed potential:

1. Cup zonal isolation
2. Swellable packer technology
3. Metal expandable well annular barrier

The final option was chosen as the most promising and work with development and qualification was initiated. [1,2]

The WAB is ultimately meant to be a part of a larger well design solution, known as Flex-Well, which can consist of up to seven different components:

1. WAB ZI – for zonal isolation
2. WAB WI – for well integrity
3. WAB LH – for liner hanger
4. WFV (Welltec Flow Valve) – for flow control
5. WDM (Welltec Data Monitor) – for data monitoring
6. WDR (Welltec Data Receiver)
7. WCS (Well Screens)

Figure 1: WAB pre-expansion

There are several versions of the WAB, but in general, it consists of three main components:

1. Liner (base pipe) with setting port
2. Expandable sleeve with elastomer sealing elements
3. End couplings with one way pressure valve [3]

It is, in simplicity, a metal sleeve, which is welded onto the base pipe (casing or liner) and is set by applying an internal pressure through the bore of the pipe with a fluid. As the internal pressure increases, the WAB sleeve expands and is able to conform to the wellbore. Any fluid can be used to pressurize the WAB, as there is a screen filter installed which ensures that no large debris will enter the annulus between the base pipe and WAB sleeve.

There are different methods available to apply pressure to the WAB. One is by using a wiper dart when cementing. As soon as the top dart has reached the landing shoe, pressure is applied and the WAB is expanded. Welltec also has its own straddle tool, called the Welltec Multi-set Injection Tool (WMIT), which can pressurize up to several WABs at the same time. Two pairs of cups are used to seal off the length that is to be pressurized. The process is initiated by dropping a ball into the tool, which seals of a channel and allows for pressure to be applied in the space between the cups. An RTTS packer can also be used to seal off the annulus below the WAB. [4]
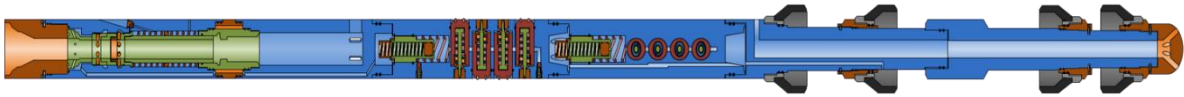
Figure 2: WMIT tool (used with permission from Welltec)

A valve block is installed in the WAB to enable pressurization of the sleeve. The block consists of a control valve and a shuttle valve, each with distinct tasks. A passage from the base pipe goes through the control valve and further into the sleeve. As soon as the final expansion pressure is reached, a shear pin breaks and the communication between the base pipe and WAB sleeve is cut. At this point, the shuttle valve is activated, which has passages to allow pressurization from either below or above the WAB (whichever annulus has the highest pressure). In this way, pressure balance is maintained across the WAB. Since there is no communication with the base pipe after the control valve has been sheared, a non-compromised barrier envelope is established. [1,5]

If any damage should happen to the WAB during deployment or installation that makes it incompetent, it is possible to cut the shear valve so that integrity and the barrier envelope is preserved.
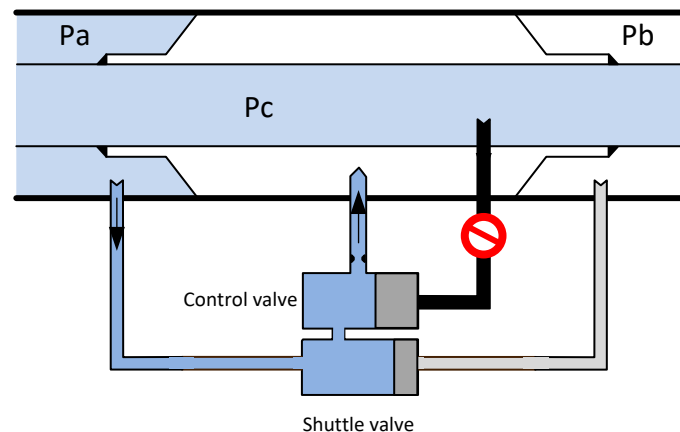
Figure 3: Valve block post-expansion (used with permission from Welltec)

At one point during expansion, the sleeve will meet the formation wall. As pressurization proceeds, expansion will continue into the formation until full expansion pressure is achieved. This is when the control valve is cut and the sleeve is pressure equalized by the annulus either above or below the WAB. Since this pressure is lower than the expansion pressure, the WAB will experience some elastic springback naturally (normally causing a 0.2% reduction in diameter). It is designed in the way that this contraction causes the elastomer seals to bulge out, making them the primary sealing components.

Due to the generally high elasticity (low Young's modulus) of a formation, it will ideally follow both the expansion and contraction, assuring that the WAB is constantly conformed to the wellbore. [2]

Note that sleeve expansion will cause some lateral contraction of the base pipe.

Simulations have shown that to withstand a differential pressure of 5000 psi, a contact stress with the formation of at least 200 psi is necessary. It will be shown later in the thesis that this is in most cases much lower than the stress necessary to damage/fracture the formation, which assures that the integrity of the well is maintained. [3,6]

The sleeve is customizable both in dimensioning and material selection, depending on the well in question and its requirements.

In summary, the process from start to finish looks like this:

1. Pressure is applied to the bore
2. Fluid goes through the screen filter and valve block
3. Expansion starts
4. Access from the bore is blocked by shearing the control valve once complete expansion pressure is reached
5. The shuttle valve "feels" the pressure from the annulus above and below the WAB and applies the highest pressure to energize the sleeve
6. WAB experiences elastic springback
7. Barrier envelope is established

2.2 WAB vs. Conventional Packers

There are several types of packers being used in the oilfield industry with different advantages and disadvantages. Some of the most prevalent ones are external casing packers, swellable elastomer packers, hydraulic set packers and hydrostatic set packers.

A packer has two main purposes, which is to seal off the annulus between the production casing and tubing, and anchor them to each other.

The WAB has several advantages compared to traditional packers:

- Can withstand higher pressures and temperatures
- Has better redundancy due to several sealing components
- Greater lifespan due to more durable materials
- Acid tolerance

2.2.1 External Casing Packers

External casing packers (ECPs) are made of flexible elastomers. They are set from bottom up and inflated through the wash pipe. They do not anchor to the formation and

movement of the string will cause damage over time. It is crucial that the integrity of the elastomers is maintained throughout its lifetime. Often several ECPs will be used for redundancy. Some of the concerns can be minimized by inflating the packer with cement instead of mud.

These kinds of packers are difficult to pressure test, and the best results are obtained through differential inflow tests. [7,8]

2.2.2 Swellable Elastomer Packers

Swellable elastomer packers are bonded onto the outside of the pipe and will start to swell as soon as they are in contact with an appropriate fluid (oil or water). They are simpler and cheaper than expandable casing packers, but have other limitations.

Having a small clearance between the packer and annulus can promote high sealing pressures (up to 4000 psi), but increases the risk of stuck pipe. It is also crucial to avoid contamination to prevent premature swelling.

Testing the swellable packers is more difficult than for ECPs, as it can take 40+ days from start to complete expansion. [7]

One of the major advantages the WAB has over these kinds of packers is that complete expansion is achieved in a number of minutes, rather than weeks. There is also no need for a special fluid to expand the sleeve, and therefore do not have to worry about swelling or contamination. The risk of getting stuck in the hole does not increase by including the WAB in the completion design either. Testing the seal is easily done by reading the data from the pressure gauges from the well data monitor (WDM, see chapter 2.3.5). It will also provide an anchor and damage due to movement is not of as much concern. [2]

2.2.3 Hydraulic Set Packers

These kinds of packers are set by sealing off the casing, for example by placing a plug or dropping a ball into the pipe. As pressure is increased inside the tubing, a setting piston is activated which sets the slips and packer element. [9]

2.2.4 Hydrostatic Set Packers

The hydrostatic set packers work in a similar way as the hydraulic set ones. The difference is that instead of being activated by a pressure differential between the tubing and annulus, they are set at a predetermined pressure with the use of an atmospheric chamber. This removes the need for plugging the casing.

Some movement will happen during installation due to piston and ballooning forces. [7]

A major disadvantage with mechanical packers like these are that they occupy a large amount of space inside the pipe and therefore restrict production and intervention. Since the WAB is placed on the outside of the pipe, this problem is eliminated. Another advantage is that it is faster to set.

2.3 Applications and Advantages

By including the WAB in the completion design of a well, a number of problems and challenges can be avoided or reduced. Some of them were introduced in the introduction of this chapter as a part of the Flex-Well system. As of now, its two main applications on the Norwegian continental shelf (NCS) are zonal isolation and cement assurance.

2.3.1 WAB as a Primary Well Barrier

The main purpose of the WAB is to function as a standalone barrier plug in the open-hole formation. The possibility of applying it in this manner helps solve a number of well integrity issues. The most significant one is that it can reduce the need for cement when placing a barrier in the well.

Cementing operations are often difficult to complete successfully due to challenges with the formation, such as fluid losses (Equivalent Circulating Density (ECD)) during placement, fracturing and contamination. The cement quality can also tend to deteriorate over time if it is exposed to harsh conditions. With the WAB, these issues can potentially be eliminated. It also works a lot faster and is easy to place at the correct depth. The seal is painlessly tested with pressure gauges installed. [10]

It has already been qualified and used successfully in this manner in an oilfield in Brazil. In Norway, however, regulations are not the same and some qualifications remain to prove that the WAB meets all the NORSOK D-010 requirements and is viable for this type of use on the NCS.

As of today, it is qualified to ISO 14310 V3 to V0 leak criteria, which is the proper standard for packers. This allows the WAB to be used as a primary well barrier on the NCS, as long as it is placed inside the previous casing with good cement behind the casing shoe. Further qualifications are being done so that it eventually can be used as a primary barrier in the open hole.

2.3.2 WAB for Zonal Isolation

Using the WAB for zonal isolation is useful either for separating different reservoir zones or for isolating shallow formations with potential inflow.

By isolating different reservoirs, it is possible to control the production from each zone through special flow valves with adjustable chokes. This is advantageous in situations where for example a zone is producing water.

Isolating shallow reservoirs can also remove the problem of sustained casing pressure (SCP). If the WAB is placed above a zone of inflow, it can prevent a pressure build up in the annulus. This is usually not an issue with onshore and platform wells, where it is possible to bleed off the pressure. In subsea wells however, this is not possible, and if the pressure build up is large enough, it can threaten the well integrity.

2.3.3 WAB for Cement Assurance

When meeting difficult cementing conditions, such as depleted or unconsolidated zones, the WAB can be used to provide a foundation. After the cement job is completed, the WAB can be expanded into the green cement and will help assure a successful cementing job.

For this application, a port collar can be installed above the WAB for contingency. In case the primary cement job fails, new cement can be pushed through the collar. This will effectively seal off the problematic zone and the WAB will function as an annular foundation for the new cement operation.

2.3.4 WAB as Liner Hanger Packer

It is possible to use the WAB as a liner hanger packer as well. Since it is qualified to the highest leak criteria (V0), it can safely be placed inside a casing in full accordance to NORSOK requirements as long as a good cement job has been executed behind the casing shoe.

2.3.5 Additional Advantages

Additional advantages of the WAB and Flex-Well system are:

- No control lines
  A Well Data Monitor (WDM) installed on the outside of the pipe measures temperature and pressure. Measurements are transferred acoustically through the pipe and read by a wireline tool. This simplifies the well design and P&A later.

- No need for tie-back
  If the WAB is expanded inside the previous casing, the casing shoe will be sealed off and a tie-back liner is not necessary.

- Simplified PP&A
  If the WAB has been placed inside a casing it can be used as a foundation for the cement that forms the permanent barrier for PP&A. This can be done without any dispensation from the authorities due to the V0 leak rate qualification.

- No perforating
  Since the production liner will not be cemented, there is also no need for perforations. Inflow control can be done with inflow control devices. Field tests have also shown that this solution with an open formation surface yields lower skin and potentially better production results.

- Time and cost saving
  Quick setting time allows for less days until first oil and simpler/no cementing operation allows for cut in expenses.

1 WAB® ZI (Welltec® Annular Barrier) – for zonal isolation
2 WAB® WI (Welltec® Annular Barrier) – for well integrity
3 WAB® LH (Welltec® Annular Barrier) – for liner hanger
4 WFV™ (Welltec® Flow Valve) – for flow control
5 WDM™ (Welltec® Data Monitoring)
6 WDR™ (Welltec® Data Receiver)
7 WCS (Well Screens)
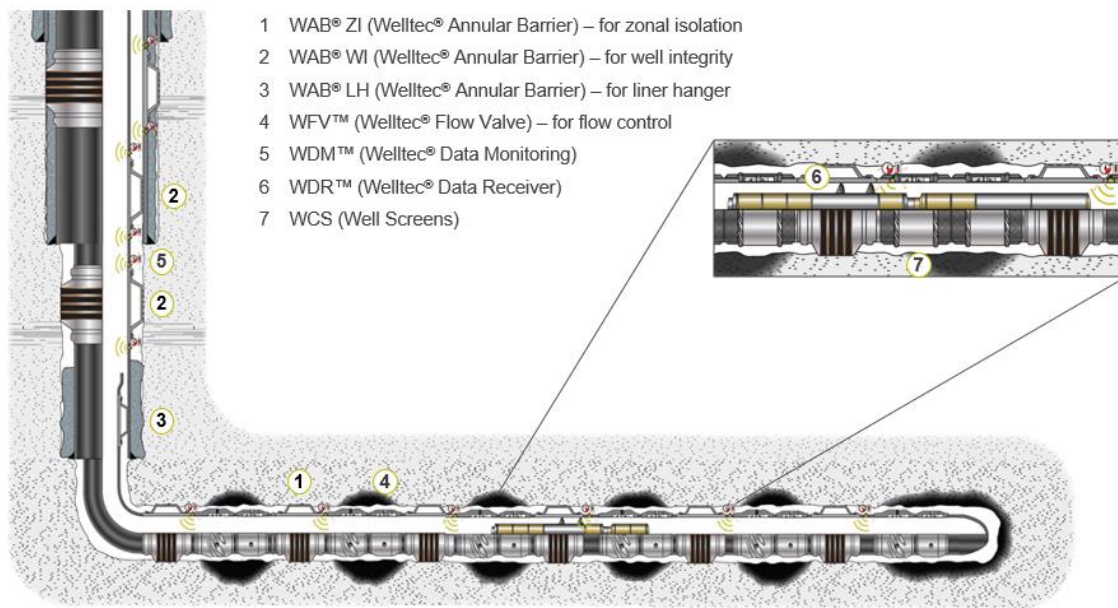
Figure 4: Illustration of the Flex-Well system (used with permission from Welltec)

2.4   Failure Modes and Qualification

Multiple failure modes were examined to obtain the proper qualifications for the WAB. To get the final ISO 14310 V0 qualification, an accelerated life test was required. This test replicated 30 years if production. [1]

The accelerated life testing consisted of various tests of the WAB elements:

- Shuttle valve failure:
  900 shuttle valve cycles were tested with varying temperatures and pressures to replicate the life of a well. Failure occurred first at a temperature of 170ºC, which is above the qualification requirements.

- Filter failure:
  Tests proved the filter can filter more than double the necessary fluid volume to expand and pressure compensate the sleeve and remain unclogged.

- Control valve failure:
  A total of 60 pins were sheared to determine the variance on shear pin rating, proved to have < 1% error margin.

- Soak test for chemical compatibility:
  Tensile tests were performed to material approval per ISO 37.

- Expansion sleeve:
  Finite Element Analysis modelling done
- Expansion sleeve test:
  Expanded into simulated formation
- Full WAB test:
  Ten cycles of ISO 14310 testing
- Axial load test:
  320,000 lbf axial anchoring force test

Another possible failure mode is that the elastomer elements will not seal properly. This issue has been addressed and lead to the inclusion of secondary seals. The likelihood for sealing can be found through stochastic analysis. One case showed that sealing could almost be guaranteed in formations with porosities lower than 15%. [1]

It is important that the WAB is able to anchor the casings to the formation. Since changes in temperature can contract or expand the pipe, it is essential that the WAB maintains an acceptable axial holding capacity.

A concern is that leakage paths will start to form at the edge of the sleeve and work themselves across the WAB to create a leakage path that eventually eradicates the barrier envelope.

Finally, if the WAB exerts large enough pressures to the surrounding formation, stresses can arise that will cause fracture and eventually failure. This will be studied closer in this thesis.

2.5 Field Cases

After its introduction in 2011, the WAB has been deployed successfully in a multitude of wells all over the world. It has been applied for all the applications mentioned in this chapter. A couple of these cases are presented.

2.5.1 WAB used for Zonal Isolation

An operator in Brazil had struggled to perform good cement jobs due to cement losses in several zones. This prevented proper zonal isolation which was necessary to avoid co-mingling production and injection.

To solve this problem, a decision was made to not cement the liner and implement four WABs in the completion instead. In this setting the WABs will also serve as the primary barrier elements.

The first was placed inside the 13 3/8" hole as a back up to the liner hanger. The remaining three were placed in the open hole between three different reservoirs, providing a barrier between each of them.

This was the first installation of a cementless liner with WABs in the world, and it proved to be successful. There was no sign of leakage, neither during water injection or acid stimulation. [5]

2.5.2 WAB Used to Prevent SCP

An operator had seen pressure buildup between the 9 5/8" and 13 3/8" casing in many wells on a Norwegian field. It was concluded that the SCP was caused by inflow from a formation right below the 13 3/8" casing shoe.

After several solutions were attempted without success, it was decided to deploy the WAB on the 9 5/8" casing string, slightly above the 13 3/8" casing shoe. It was required that the primary cementing job on the 13 3/8" casing was of high quality for this solution to work properly.

As soon as this was done, pressure was gradually built up in the well, which expanded the WAB. The seal was pressure tested and isolation and barrier verification was confirmed.

In this case, the WAB acts as a part of the secondary well barrier envelope. [5]

3. Basic Theory

In this chapter, relevant theory will be explained in simplicity to give the reader an understanding of the underlying mechanisms of further work in the thesis.

3.1   Stress

When a solid object is exposed to a force, stress arises in the system. If the force is acting through the cross section, stress is defined as:

$$\sigma = \frac{F}{A}$$

(3.1)

where σ is stress (Pa), F is the force (N) and A is the cross-sectional area (m^2).

This type of stress is called normal stress, and is one of the two stress types that can arise on a surface of a body. The second one is called shear stress (τ), which acts along the plane of the surface.

To give the most accurate description of the stress state at a specific point, it is necessary to define a *stress tensor*. The tensor a matrix given by nine stress components, three normal and six shear components. If the associated coordinate system is rotated, the stress components are rotated as well. In that case, stress transformations must be carried out to calculate the new magnitudes and orientations.

When stresses are transformed, the definition of stress is made more complicated. This problem can be avoided if the coordinate system is rotated in such a manner that all shear stresses disappear. Once that is done, only normal stresses remain and are given the name *principal stresses*. The principal stresses are of great importance when studying failure of a material, as they represent the maximum and minimum stresses in the system. [11]

If the stress components are independent of z and $\sigma_z = \tau_{xz} = \tau_{yz} = 0$, the system is said to be in a *plane stress* condition. The indices refer to the Cartesian coordinate system. The first letter defines the axis normal to the plane on which the stress acts and the second letter defines the direction of the stress component ($\sigma_z = \sigma_{zz}$). [12]

Beware that in rock mechanics, compressive stresses are positive and tensional stresses are negative, opposite to many other engineering fields. This is because most stresses in this field are compressive. In this thesis, the classic approach will be taken, defining tensional stresses and strains as positive and compressive stresses and strains as negative.

3.2   Strain

As an object is subjected to a load, it will experience deformation and/or displacement. The deformation of an object is represented by *strain*.
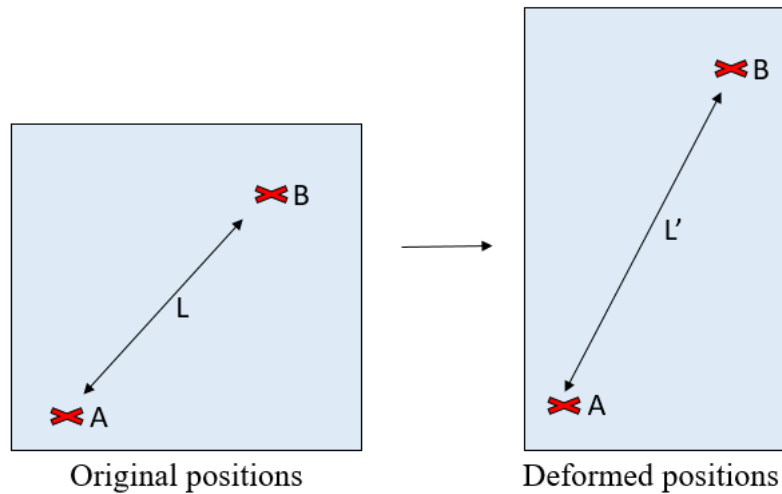
Figure 5: Deformation of an object

It is a dimensionless parameter, defined by its change in length divided by its original length:

$$\varepsilon = \frac{L' - L}{L} = \frac{\Delta L}{L} \tag{3.2}$$

where ε is the strain, L' is the new deformed length and L is the original length.

This formulation of strain is known as *engineering strain*. Another definition used is known as *scientific strain*, where the actual dimension at a certain time is used, not the original dimension.

Be aware that eq. 3.2 is only valid for small deformations. For larger strains, different expressions are necessary. [11]

If $\varepsilon_z = \varepsilon_{xz} = \varepsilon_{yz} = 0$, the strain condition is known as *plane strain*. "In this case all cross-sections along a given axis are in the same condition and there is no displacement along the axis." [12]

3.3   Rock Mechanics

During drilling operations, it is important to be aware of the properties of the various formations that are present. A natural, static, stress state is present in the rock, known as the *in-situ stress*. Drilling into the formation changes the in-situ stress in the near wellbore area, which can cause a number of challenges.

A wide range of processes, such as erosion, transportation and deposition, constructs the rock properties. Having an understanding of these processes is therefore helpful when establishing the features of the rock. [12]

Because rocks are made of various grains of different sizes and shapes cemented together, they are anisotropic, which is to say that no matter the orientation of the applied stress, the response of the material remains indifferent. They are also non-homogeneous and follow a non-linear relation.

However, knowledge of the different rock parameters is usually limited. Because of this, the formation is often assumed isotropic, homogenous and linear-elastic when modeling. This can have a large effect on the resulting fracture pressure of the formation. The most anisotropic rock (Arkansas Sandstone) has a fracture pressure that is 11% larger than its isotropic equivalent. [11]

At times, there will be some spaces, also known as pores, in between the grains and cement. The pores are saturated with either fluids or gasses, and as they are buried deeper below the surface, a pressure build-up is created. The resulting pressure is called *pore pressure*.

If the fluid inside the pores have a migration route to the surface, the pore pressure will be equal to the hydrostatic pressure. For various reasons, this is at many times not the case and the pressure will be higher (called abnormal pressure or overpressure). Overpressure can make a field more yielding, but it also represents a potential risk and wellbore stability issues are more common. Formations with low permeability, such as clays and shaly zones, are more prone to being overpressured. [12]

Some of the formation properties that will affect the resulting stresses are the Poisson's ratio (v), Young's modulus (E) and Biot's constant (β).

The Poisson's ratio is the relationship between the lateral expansion of a material and the lengthwise contraction of a material. It is given by:

$$v = -\frac{\varepsilon_y}{\varepsilon_x} \tag{3.3}$$

The Young's modulus, also known as the Modulus of Elasticity, represents the stiffness of a material. It is given by:

$$E = \frac{\sigma_x}{\varepsilon_x} \tag{3.4}$$

The Biot's constant is a scaling constant, it is explained further in chapter 5.2.

If the rock in question is assumed to be isotropic and homogenous, the Poisson's ratio and Young's modulus are considered to be scalar. That is to say that they are of the same magnitude in all directions. This simplification may not be far off for the Poisson's

ratio, but the Young's modulus is generally greatly anisotropic. The effect of these will be shown later in the thesis.

The strength of the rock is dependent on the cementing, and interlocking/orientation of the grains. It is specified by its tensile, compressive, shear and impact strength. Two other important properties in rock modelling is the internal friction (angle and coefficient) and cohesion (inherent shear strength). [11]

3.4   Well Stability

During drilling and production of oil and gas, it is of utter importance to preserve stability of the wellbore. Collapse and fracture of the well are two of the most critical stability issues, but they are just a couple of many stability challenges that can arise during the life of a well. Most of these issues are avoidable to some degree through diligent planning. This can be a tedious process however, as they are influenced by a multitude of factors, ranging anywhere from well deviation to the chemical interaction between the formation and drilling mud.

In this thesis, wellbore stability with a focus on failure due to fracture is considered. It is common that the pressure in the well is higher than the pore pressure, a condition known as overpressure, but at one point the pressure is too high and the formation will start to fracture. This is due to the well pressure causing a reduction in the circumferential stress, finally making it lower than the tensile strength of the formation. It is therefore important to keep a balance between the stresses of the overburden and the stresses created in the borehole. [11] [13]

4. Thick-Walled Cylinder and Autofrettage

In this chapter, the equations for stresses in a cylinder are introduced. They are then used to develop an equation for the pressure that arises between the WAB and the formation.

4.1　Cylinder Theory

As pressure is built up inside the WAB, certain stresses will arise on the wall of the sleeve. Equations for these stresses need to be known to find the pressure that the WAB exerts on the borehole wall.

Generally, hollow, circular cylinders are split into two categories; thick and thin walled. They have the following criteria:

Thin walled if:

$$t < \frac{1}{10}a \tag{4.1}$$

Thick walled if:

$$t > \frac{1}{10}a \tag{4.2}$$

Where t is the thickness and a is the inner radius. [14]

Note that the equations for a thick wall cylinder are applicable for thin walled cylinders, but not vice versa. Only stresses in a thick-walled cylinder are studied further, as they are the ones that contribute to the final pressure equation.

The stresses in a cylinder cannot be expressed with Cartesian coordinates, cylindrical coordinates need to be used instead. In this case, the stress state at a point in a cylinder is given by the *radial* (r), *tangential* (θ) and *axial* (z) stresses. [12]
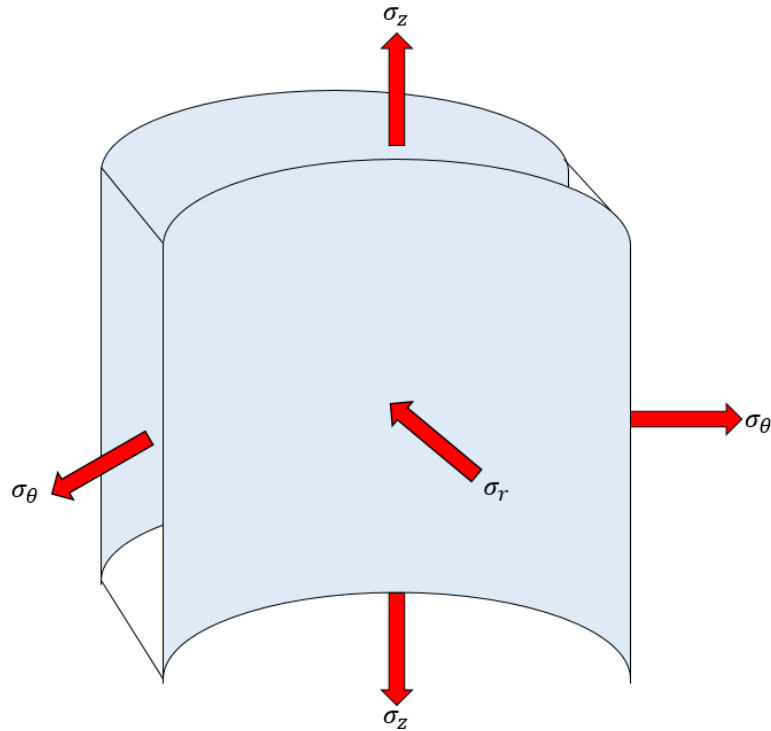
Figure 6: Stresses in a cylinder wall

4.2 Stresses in a Thick-Walled Cylinder

To calculate the stress components of a hollow, closed thick-wall cylinder, assuming no temperature change ($\Delta T = 0$), three equations are presented. They are known as the Lamé Equations. [14]

Radial stress:

$$\sigma_r = \frac{p_1 a^2 - p_2 b^2}{b^2 - a^2} - \frac{a^2 b^2}{r^2(b^2 - a^2)}(p_1 - p_2) \tag{4.3}$$

Tangential stress:

$$\sigma_\theta = \frac{p_1 a^2 - p_2 b^2}{b^2 - a^2} + \frac{a^2 b^2}{r^2(b^2 - a^2)}(p_1 - p_2) \tag{4.4}$$

Axial stress for open cylinder:

$$\sigma_z = 2v \frac{p_1 a^2 - p_2 b^2}{b^2 - a^2} \tag{4.5}$$

Where the variables are:

p_1	Internal pressure
p_2	External pressure
a	Inner radius
b	Outer radius
r	Radial coordinate
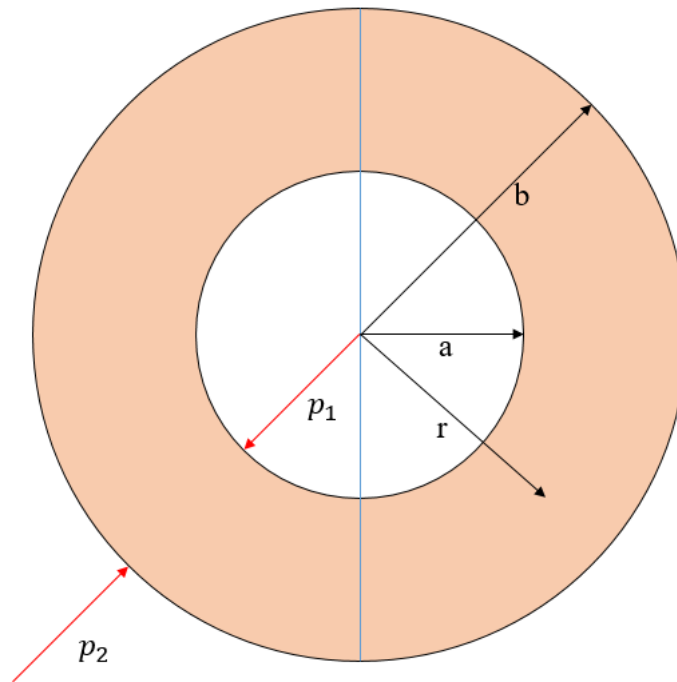
Figure 7: Cylinder schematic

See appendix A for the derivation of the Lamé equations.

4.3   Shrink Pressure

The WAB is imagined to be one cylinder and the formation to be another. As the WAB expands into the formation, a *shrink pressure* (p_s) is created between the two cylinders. A similar process, known as autofrettage, is applied in industries to strengthen thick walled cylinders.

In an autofrettage process, an inner cylinder is inserted inside another outer cylinder. The outer radius of the inner cylinder is marginally larger than the inner radius of the outer cylinder. The inner cylinder is cooled (which makes it contract) and/or the outer cylinder is heated (which makes it expand). It will then be possible to slip the inner cylinder inside the outer cylinder. As they reach a common temperature, a shrink pressure is created between the surfaces of the cylinders, introducing residual stresses

(stresses that are still present after loading forces have been removed) in the cylinders. As a result, the composite cylinders strength increases. [15] [16]

Note that the shrink pressure in this case is the pressure created between the metal elements of the WAB and the formation, not the elastomer seals. Simulations have shown, however, that the metal rings are the components that will create the largest effective stresses during the setting process, and it is therefore correct to study these. [2] [3]

4.3.1 Development of the Shrink Pressure Equation

To develop the equation for the shrink pressure that arises between the cylinders, the equation for the radial displacement of a cylinder under pressure is considered.

The equation for radial displacement is derived through a combination of five different equations. They are the three equations for stress components in a closed cylinder (Lamé's equations), stress-strain-temperature relation and strain-displacement relation for hoop strain.

The strain-displacement relation for a thick-walled cylinder for extensional hoop strain is defined as:

$$\varepsilon_\theta = \frac{u}{r} \tag{4.6}$$

where $u = u(r,z)$ denotes displacement component in r and z directions, respectively.

The stress-strain-temperature relation for hoop strain, assuming no axial stress, is: [3] [15]

$$\varepsilon_\theta = \frac{1}{E}[\sigma_\theta - v(\sigma_r + \sigma_z)] \tag{4.7}$$

By applying this, and combining eq. 4.6 and eq. 4.7, the equation for the radial displacement becomes:

$$u = r\varepsilon_\theta = \frac{r}{E}[\sigma_\theta - v\sigma_r] \tag{4.8}$$

$$u = \frac{r}{E}\left[\frac{p_1 a^2 - p_2 b^2}{b^2 - a^2} + \frac{a^2 b^2}{r^2(b^2 - a^2)}(p_1 - p_2) - v\frac{p_1 a^2 - p_2 b^2}{b^2 - a^2} + v\frac{a^2 b^2}{r^2(b^2 - a^2)}(p_1 - p_2)\right] \tag{4.9}$$

$$u = \frac{r}{E(b^2 - a^2)} \left[p_1 a^2 - p_2 b^2 - v p_1 a^2 + v p_2 b^2 + \frac{a^2 b^2}{r^2}(p_1 - p_2) \right.$$
$$\left. + v \frac{a^2 b^2}{r^2}(p_1 - p_2) \right] \quad\quad (4.10)$$

The final equation for the radial displacement for an open cylinder is:

$$u = \frac{r}{E(b^2 - a^2)} \left[(1-v)(p_1 a^2 - p_2 b^2) + \frac{(1+v)a^2 b^2}{r^2}(p_1 - p_2) \right] \quad\quad (4.11)$$

If the initial difference of the outer radius of the inner cylinder (WAB), and the inner radius of the outer cylinder (formation) is known, it is possible to calculate the shrink pressure. When the equilibrium is met after expansion, both of the cylinders will have experienced a radial displacement and the sum of this displacement (Δu) has to be equal to the initial difference. [15]

First, the variables that are used are defined.

For the inner cylinder:

a	a
b	c_i
p_1	0
p_2	p_s
E	E_i
v	v_i

For the outer cylinder:

a	c_o
b	b
p_1	p_s
p_2	0
E	E_o
v	v_o

where c_o is the inner radius of the outer cylinder and c_i is the outer radius of the inner cylinder.
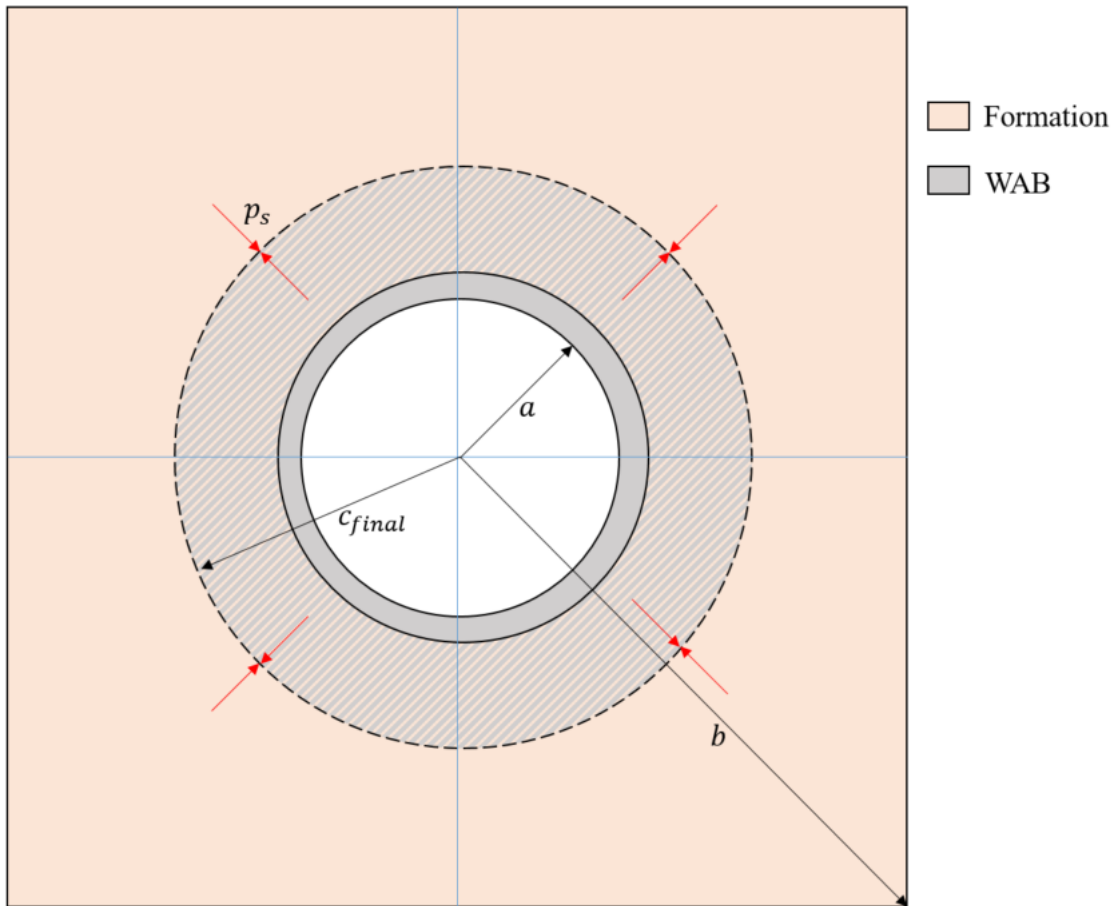
Figure 8: Shrink pressure schematic

The first steps to derive the equation for the shrink pressure is to solve eq. 4.11 for the inner and outer cylinder.

Radial displacement for the inner cylinder, u_i:

$$u_i : r = b = c_i$$

$$u_i = \frac{c_i}{E_i(c_i^2 - a^2)}\left[(1 - v_i)(0 - p_s c_i^2) + (1 + v_i)\frac{a^2 c_i^2}{c_i^2}(0 - p_s)\right] \tag{4.12}$$

Simplify:

$$u_i = \frac{c_i}{E_i(c_i^2 - a^2)}[-(1 - v_i)c_i^2 - (1 + v_i)a^2]p_s \tag{4.13}$$

Radial displacement for the outer cylinder, u_o:

$$u_o : r = a = c_o$$

$$u_o = \frac{c_o}{E_o(b^2 - c_o^2)}[(1 - v_o)(p_s c_o^2 - 0) + (1 + v_o)\frac{c_o^2 b^2}{c_o^2}(p_s - 0)] \qquad (4.14)$$

Simplify:

$$u_o = \frac{c_o}{E_o(b^2 - c_o^2)}[(1 - v_o)c_o^2 + (1 + v_o)b^2]p_s \qquad (4.15)$$

The next steps are to find the equation for *Δu* and then solve it for p_s:

$$\Delta u = u_o - u_i \qquad (4.16)$$

$$\Delta u = \frac{c_o}{E_o(b^2 - c_o^2)}[(1 - v_o)c_o^2 + (1 + v_o)b^2]p_s$$
$$- \frac{c_i}{E_i(c_i^2 - a^2)}[-(1 - v_i)c_i^2 - (1 + v_i)a^2]p_s \qquad (4.175)$$

$$p_s = \frac{\Delta u}{\frac{c_o}{E_o(b^2 - c_o^2)}[(1 - v_o)c_o^2 + (1 + v_o)b^2] + \frac{c_i}{E_i(c_i^2 - a^2)}[(1 - v_i)c_i^2 + (1 + v_i)a^2]} \qquad (4.18)$$

However, if an expansion of the inner cylinder is considered using eq. 4.18 as it is, it will appear as if the thickness of the sleeve expands, thus increasing its volume. This is obviously not the case and needs to be accounted for in the equation.

Since the inner radius increases by the same amount as the outer radius, *a* is expressed as:

$$a = c_i - t \qquad (4.19)$$

Inserting this yields the final equation for the shrink pressure:

$$p_s = \Delta u *$$
$$\frac{1}{\frac{c_o}{E_o(b^2 - c_o^2)}[(1 - v_o)c_o^2 + (1 + v_o)b^2] + \frac{c_i}{E_i[c_i^2 - (c_i - t)^2]}[(1 - v_i)c_i^2 + (1 + v_i)(c_i - t)^2]} \qquad (4.21)$$

As can be seen, the resulting pressure is highly dependent on how large the expansion into the formation is. It will be shown later in the thesis that even very small values for

Δu will give high pressures. Further on in the thesis this pressure will be applied in well fracture calculations.

The reader should be aware that *Δu* is the sum of the displacements. If the shrink pressure is inserted in eq. 4.13, the result will give a negative value for u_i. This is because the specifications/assumptions that are made to find p_s will cause the outer radius of the WAB to shrink and the inner radius of the formation to expand. They will reach a final common radius, given by:

$$c_{final} = u_o + c_o = u_i + c_i \tag{4.22}$$

This is due to the fact that usually in calculations for autofrettage, the measurements before expansion/contraction of the cylinders are known. In these calculations, the sum of the displacements is assumed to take on a specific value, which makes it look like the WAB has an original outer radius equal to c_i. This is not the case, but the assumptions should still be valid to find a shrink pressure.

An example follows, to illustrate what this will look like.

4.3.2 Shrink Pressure Example
Assume a WAB and a wellbore with these specifications:

	WAB	Formation
Outer radius (m)	0.156	10000
Inner radius (m)	0.144	0.1556
Young's modulus (MPa)	$200*10^3$	$15.05*10^3$
Poisson's ratio	0.3	0.225

In this case, it is assumed that the sum of the displacements equals 0.4 mm. This means that in a hole with a radius of 0.1556 m (12 ¼"), the outer radius (c_i) of the WAB must take a value of 0.156 m.

However, as the WAB expands into the formation, c_i will never reach this value. The expansion of the WAB and formation will stop at a common radius (c_{final}) which will be a little smaller than c_i and a little larger than c_o.

Applying eq. 4.20, yields a shrink pressure of 18.021 MPa. Inserting this in eqs. 4.15 and 4.13 respectively, gives a u_o of 0.2282 mm and a u_i of -0.1717 mm. The final radius of the cylinders is 0.1558 m.

Notice also how u_o - u_i gives a value of 0.4 mm.

4.4　Contact Stress

The contact stress between the WAB and the formation is given by the radial stress that arises due to the pressurization of the WAB. Boundary conditions from the Lamé equations say that the radial stress in the system is equal to the pressure exerted on the wall. This implies that $\sigma_r = p_s$.

5. Wellbore Stress and Fracturing

In this chapter, the stresses in formations and wellbores will be studied. Equations to calculate the well stresses and pressures are presented. They will be used in combination with the shrink pressure to determine if the well will fracture around the WAB.

5.1   In-Situ Stress

The in-situ stress state in a formation consists of three orthogonal principal stresses (maximum, intermediate and minimum) as well as the pore pressure. They are generally considered to be in the vertical and horizontal directions. [11]

When studying wellbore fracture, these pressures and stresses including the hydrostatic pressure from the fluid column in the annulus must be taken into consideration. In this case, the pressure the WAB exerts on the borehole wall should be included in the calculations as well. [12]

Excluding certain cases, such as where the stress state has been altered due to tectonic activity, the vertical stress can justifiably, and practically, be considered as a principal stress. This is due to gravity working in the same direction, towards the center of the Earth. The two corresponding principal stresses will then be the horizontal stresses. However, this will not be the case at shallow depths since the surface is stress free.

The three principal stresses are known as overburden (σ_v), maximum horizontal (σ_H) and minimum horizontal (σ_h) stress. These stresses are normally compressive and increase with depth. [11]
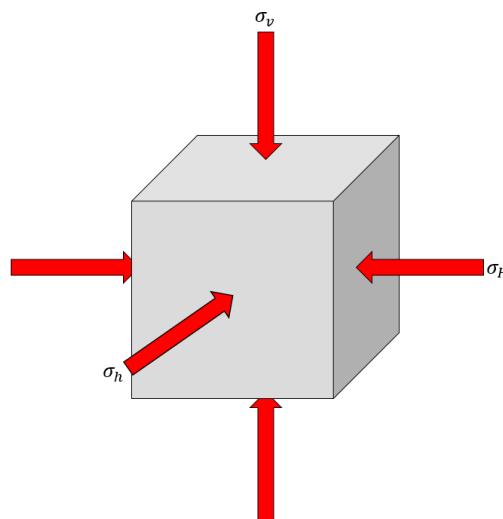

Figure 9: Principal stresses

The overburden stress is primarily caused by the weight of the formation and fluids above and increases regularly with depth, but some tectonic settings can have an effect as well. The two horizontal stresses are a product of the overburden stress. Depending on the Poisson's ratio of the formation, the overburden will attempt to broaden the rock laterally to some degree. The presence of surrounding materials will restrain this movement, and the horizontal lateral stresses arise. Note that changes in temperature will affect the stresses, but that is not considered in this thesis. [11] [12]

In a vertical borehole, the maximum principal stress is typically represented by the vertical stress (overburden stress), and the intermediate and minimum stresses are represented by the two horizontal stresses. The horizontal stresses are usually of different magnitudes, due to tectonic stresses, but have traditionally been assumed to be equal. [11]

It is difficult to correctly determine the in-situ principal stresses mathematically. While it is possible to make some assumptions, and estimate the stresses, they should always be measured to be certain. There are two ways to measure the magnitude of the in-situ stresses, directly (experimentally) and indirectly (analytically). Within these, there are several methods (such as cross dipole log, leak off test, mini-frac test), but they will not be covered in this thesis. Analyzing traces from fractures is currently the only way to assess the direction of the principal in-situ stresses. [11]

This means that while equations for calculating the stresses exists, they should always be applied with caution. Even more so at shallow depths, where residual or structural stresses may be present that can cause large horizontal stresses.

Pore pressure works in all directions and therefore only affects the normal stresses in the formation. This will effectively relieve some of the stress on the rock matrix as it helps carry part of the total weight of the overburden.

Direct measurement of the pore pressure is only possible in permeable formations. There are currently no accurate methods of estimating the pore pressure in impermeable formations, such as shales or clays. [11] [12]

5.2 Effective Stress

Effective stress in a formation is defined as the total stress minus the pore pressure. A considerable amount of data supports the theory that porous, saturated and permeable rocks adhere to an effective stress law. Insight of the pore pressure is therefore essential when doing rock modelling. [12]

The total stress in a system is given by the effective stress plus the pore pressure (p_p):

$$\sigma = \sigma' + p_p \qquad (5.1)$$

A scaling constant/correction factor to the pore pressure is usually included, known as the Biot's constant. The effective stress is then:

$$\sigma' = \sigma - \beta p_p \tag{5.2}$$

Where β is given by:

$$\beta = 1 - \frac{E}{E_i}\frac{1 - 2v_i}{1 - 2v} = 1 - \frac{\text{Porous Matter}}{\text{Interpore Material}} \tag{5.3}$$

i refers to the inter-pore material. The constant usually takes a value of 0.8-1. In fragile rocks, it will be closer to 1. [11] [12]

Terzaghi made two arguments that led to the development of an effective stress law. They said that:

1. "Increasing the external hydrostatic pressure produces the same volume change of the material as reducing the pore pressure with the same amount"
2. "The shear strength depends only on the difference between the normal stress σ and pore pressure p_p"

Argument number 2 suggests that it is the effective stress that causes failure, not the total stress. This will be implemented when calculating the fracture pressure later. [12]

5.3   In-Situ Stress Equations
A variety of equations exists to calculate the in-situ stresses of a formation. A few of them will be introduced here and applied later during fracture calculations.

5.3.1 Overburden Stress
One can find the overburden stress in a formation with inconsistent densities through this equation:

$$\sigma_v = \int_0^d \rho_b(h)g\,dh \tag{5.4}$$

where ρ_b is the formation bulk density (lb/ft^3), g is the gravitational constant (32.175 ft/s^2), h is the vertical thickness of the rock formation (ft) and d is the rock formation depth (ft). $d = 0$ is at the Earth's surface.

It is not unusual to see an overburden averaging between 1.8-2.2 g/cm^3, which yields an increase in overburden stress of approximately -20 MPa/km.

Formation bulk density can also be calculated, using this equation:

$$\rho_b = \rho_r(1 - \emptyset) + \rho_f\emptyset \tag{5.5}$$

where ρ_r is the rock grain density (kg/m³), ρ_f (kg/m³) is the fluid density and $\emptyset$ is the porosity of the formation.

If the average formation density and pore pressure gradient is known, eq. 5.4 can be reformulated to:

$$\sigma_v = \rho_b g d = \gamma_b d \tag{5.6}$$

where γ_b is the rock formation specific weight (lbf/ft³).

To get the result in psi, the relation $\gamma_b = \gamma * \gamma_w$ is applied, where γ_w is the specific weight of water (lbf/ft³) and γ is the formation specific gravity (s.g.). After unit conversion, the equation turns out to be:

$$\sigma_v = 0.434\gamma d \tag{5.7}$$

where d is the depth in feet.

However, since the overburden stress is compressive, it must be given a negative value. Thus, making the equation:

$$\sigma_v = -0.434\gamma d \tag{5.8}$$

Usually, it will not be necessary to calculate the overburden stress, as it is easily obtained from density logs. [11]

5.3.2 Pore Pressure

When the pore pressure is given by the hydrostatic (normal pore pressure, p_{pn}), the equation is:

$$p_{pn} = -\int_0^d \rho_{pf}(h)g d h \tag{5.9}$$

where ρ_{pf} is the density of the pore fluid (kg/m³).

A normal pore pressure equals a pressure gradient of approximately -10 MPa/km. In this situation, the pores of the formation will typically be occupied by a brine with a density of 1.03-1.07 g/cm³. This indicates that the effective overburden stress also will increase by 10 MPa/km. [12,13]

If a well has a pore pressure gradient higher than -0.8 psi/ft. and/or has a bottom hole temperature higher than 150ºC, it is said to be a high pressure, high temperature (HPHT) well. [17]

5.3.3 Horizontal Stress

Avasthi *et al.* introduced an equation based on the Biot's constant, Poisson's ratio, overburden stress and pore pressure (p_p) to estimate the in-situ horizontal stress:

$$\sigma_h = \frac{v}{1-v}(\sigma_v - \beta p_p) + \beta p_p \tag{5.10}$$

The horizontal stresses are also compressive, and since the overburden stress and pore pressure also has been assigned a negative value, a few of modifications must be done:

$$\sigma_h = -\left[\frac{v}{1-v}(-\sigma_v + \beta p_p) - \beta p_p\right] \tag{5.11}$$

Breckels and van Eekelen utilized fracturing data from several wells to develop a relation between the depth and horizontal stress.

For depths above 3500 meters:

$$\sigma_h = -\left[0.0053 d^{1.145} + 0.46(p_p - p_{pn})\right] \tag{5.12}$$

For depths below 3500 meters:

$$\sigma_h = -\left[0.0264 d - 31.7 + 0.46(p_p - p_{pn})\right] \tag{5.13}$$

If there is an abnormal pore pressure present, it will be accounted for in these equations. [12]

As mentioned previously, the stresses will usually have unequal magnitudes, but additional horizontal stresses are difficult to calculate and should be assumed. They are not as easily measured as the overburden stress either. It is common to assume that σ_h = σ_H, but this is only the case when the horizontal stresses are purely caused by the overburden. [11]

5.4   Formation Properties after Drilling

Once drilling starts, the in-situ stresses are disturbed and a new set of stresses are established around the borehole. In-situ stresses are still present, but at a further distance into the formation. Removal of rock material creates an open surface in the

formation, and eliminates its natural confinement properties. This leads to a reduction in strength and eventually an inelastic and time dependent failure. [11]

Pore pressure will also be affected during a drilling operation, as well as the cohesive strength and capillary forces of the rock. [12]

Usually, only the fluid pressure supports the wellbore surface. In this case, the WAB will also provide some support. The stresses that the fluid column and WAB exerts, will not be equal to the stresses that were present in the undisturbed formation.

As pressure builds up, it will eventually reach a magnitude where some volumetric elastic deformation of the wellbore will occur. This expansion continues until the stresses are too large for the borehole to support. At this point the fracturing process is initiated. [11]

5.5   Formation Fracturing

When studying fracture, primarily tensile strength is of interest. This is due to its low magnitude, compared to the compressive strength. For this reason, it is much more likely that failure will occur in tension rather than in compression.

It has been common to use knowledge form previous wells and develop empirical correlations to predict the pore and formation fracture pressure. New methods have been developed over the years, but some of the correlations are still relevant.

The formation fracture gradient is the pressure that is necessary to induce fracture at a certain depth. The indirect and direct measurement methods briefly mentioned previously are also applied here to determine the gradient. Laboratory testing is also an alternative to determine the rock strength.

5.5.1   Fracturing Mechanism

A *stress intensity factor* represents the stress concentration at the tip of a crack at a given loading. As soon as the factor exceeds a certain value, known as the *fracture toughness*, cracks will start to develop. A crack is defined as any opening in the rock that has one or two dimensions much smaller than the third. The width to length ratio is typically 10^{-3} to 10^{-5}.

Once the effective strength of a rock is exceeded, a failure will occur across some plane in the formation. The failure will usually split along one, or very few, fracture planes normal to the direction of the tensile stress. This makes tensile failure a localized and inhomogeneous process, and the larger the cracks are, the faster they will grow. [18]

As the formation starts to yield due to excessive overpressure, small cracks will initially be generated. Continuing to increase the pressure will eventually cause a plastic

deformation of the formation and growth of cracks. At one point the cracks will abruptly widen. This can cause a severe loss of fluid into the formation. [11]
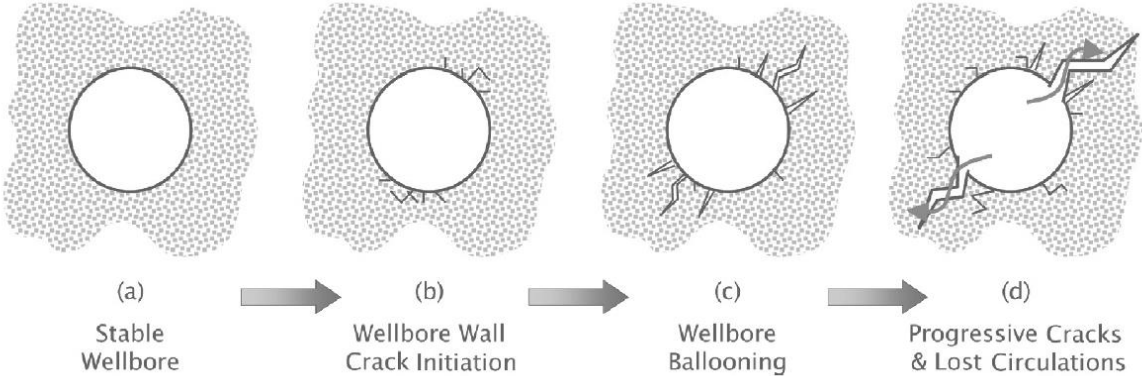
Figure 10: Sequence of fracture failure [4]

Fracturing is divided into three separate modes; Mode I (opening), Mode II (sliding) or Mode III (tearing). It is known as a *mixed mode* if a combination of any of these modes form the fracture. [19]
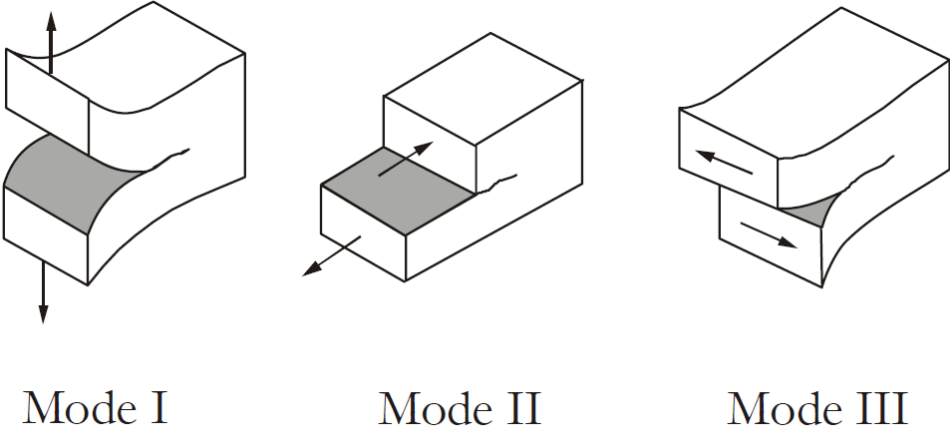
Figure 11: Fracturing modes [18]

5.5.2 Tensile Strength

In many cases, tensile strength can be assumed equal to zero. This is because of preexisting micro-cracks and fissures in the rock. With this comes the implication that once the tensile rock stress goes from a state of compression to tension, fracturing is initiated.

With mechanics, it is possible to calculate the resulting tensile stress on the formation and determine if failure will occur or not. As soon as the sum of the stresses on the

borehole wall get a positive value (tension), it is assumed that failure has initiated. In this case the stress from the WAB and fluid column should be added to the horizontal stress.

5.5.3 Fracture Pressure

Aadnøy [11] introduced this equation for wellbore fracture, assuming a vertical borehole, oriented in a principal stress direction and a normal fault stress state:

$$p_{wf} = 3\sigma_h - \sigma_H - p_p \tag{5.14}$$

Another equation was also developed, that will lead to a similar expression.

Assuming a plane strain condition, the radial strain in terms of effective stress and temperature is given by:

$$\varepsilon_\theta = \frac{1}{E}[(1 - v^2)\sigma'_\theta - v(1 + v)\sigma'_r] + (1 + v)\alpha\Delta T \tag{5.15}$$

The effective radial stress in the well can be related to the volumetric strain as:

$$\Delta P = K\left[\frac{\varepsilon_r}{\varepsilon_\theta} + 1 + \frac{\varepsilon_z}{\varepsilon_\theta}\right]\varepsilon_\theta \tag{5.16}$$

where K is the bulk modulus of the formation.

In the expanding borehole, the Poisson's ratio is given by:

$$v = \frac{\varepsilon_\theta}{\varepsilon_r} \tag{5.17}$$

By inserting eq. 5.15 and 5.17 into eq. 5.16, the effective differential pressure is given by:

$$\begin{aligned}
\Delta P &= p_{wf} - p_p \\
&= \frac{K}{E}\left[1 + \frac{1}{v} + 0\right]\{(1 - v^2)\sigma'_\theta - v(v + 1)\sigma'_r\} \\
&\quad + K\frac{(1 + v)^2}{v}\alpha\Delta T
\end{aligned} \tag{5.18}$$

where:

$$\frac{E}{K} = 3(1 - 2v) \tag{5.19}$$

The connection between the well pressure and effective borehole stress will then be:

$$\Delta P = \frac{1+v}{3v(1-2v)}[(1-v^2)\sigma'_\theta - v(v+1)\sigma'] + K\frac{(1+v)^2}{v}\alpha\Delta T \tag{5.20}$$

The hoop stress in the direction of a fracture, in a vertical wellbore is given by:

$$\sigma'_\theta = 3\sigma_h - \sigma_H - p_w - p_p \tag{5.21}$$
$$\sigma'_\theta = p_w - p_p \tag{5.22}$$

For a case where the fracturing pressure is larger than the pore pressure, eq. 5.20 can be reformulated to:

$$p_{wf} = \frac{(1+v)(1-v^2)}{3v(1-2v)+(1+v)^2}(3\sigma_h - \sigma_H - 2p_p) + p_p$$
$$+ \frac{(1+v)^2}{3v(1-2v)+(1+v)^2}E\alpha\Delta T \tag{5.23}$$

Next, assume that the normal stresses on the wellbore wall are equal, so:

$$3\sigma_h - \sigma_H - 2p_p = 2\sigma - 2p_p \tag{5.24}$$

By setting the Poisson's ratio equal to zero and removing the temperature effect, the wellbore fracture pressure is given by:

$$p_{wf} = 2\sigma_h - p_p \tag{5.25}$$

This is the equation is widely used in the industry. If the maximum and minimum horizontal stresses are assumed to be equal, this is also what eq. 5.14 will look like. [11, appendix B]

5.6 WAB Pressure Window

Fracture of the wellbore will initiate as soon as the sum of p_f, p_s and p_{wf} become zero. The maximum shrink pressure ($p_{s,max}$) is found by subtracting the hydrostatic pressure exerted by the fluid column (p_f) from the additive inverse of the fracture pressure:

$$p_{s,max} = -p_{wf} - p_f \tag{5.26}$$

Where p_f is given by:

$$p_f = \rho_f g d \tag{5.27}$$

As long as the shrink pressure is between 0-$p_{s,max}$, the well will remain unfractured. This does not mean that the well will not be damaged. Crack initiation may still occur, depending on the ratio between the formation pore pressure and overbalance in the well
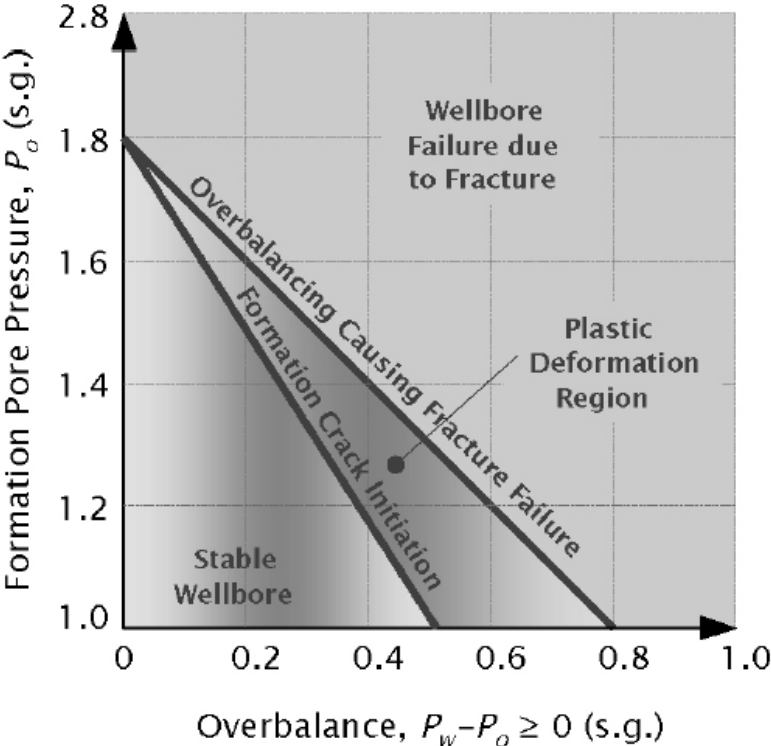
Figure 12: Wellbore failure due to fracture [11]

6. Formation Cases

In this chapter, the interaction between the WAB and various formation types will be investigated.

Eq. 5.7 is used to calculate the overburden stress in psi. It is then converted to MPa for further use. Then the horizontal stress is calculated using eq. 5.10. The fluid column pressure and pore pressure are easily calculated and will remain constant for every case (except the pore pressure in 6.5).

Once these are known, the well fracturing pressure is found by applying eq. 5.25 and the corresponding maximum shrink pressure is found by eq. 5.26.

Lastly, the maximum allowable radial deformation is found by solving eq. 4.20 for Δu and inserting the maximum shrink pressure.

Be aware that properties may vary from rock sample to rock sample, so they are often given in intervals. The average of these intervals (in the parentheses) is then applied in the calculations. Values are collected from appendix A in Fjær [12].

A 12 ¼" hole is chosen as an example, with a 9 5/8" casing at 3000-meter depth. The properties of the well are as follows:

Outer radius	10000 m
Inner radius	0.1556 m
Pore pressure gradient	-10.2 MPa/km / -0.45 psi/ft
Depth	3000 m / 9843 ft
Well fluid density	877 kg/m^3

WAB properties:

Thickness	12 mm
Young's modulus	200 * 10^3 MPa
Poisson's ratio	0.3

The pore pressure at the specified depth is:

$$p_p = -0.45 \frac{\text{psi}}{\text{ft}} * 9843 \text{ ft} = 4429 \text{ psi} * 6894.4 \, ^{Pa}/_{psi} = -30.54 \text{ MPa} \qquad (6.1)$$

The pressure exerted by the fluid column is:

$$p_w = 877 \frac{\text{kg}}{\text{m}^3} * \frac{9.81 \text{ m}}{\text{s}^2} * 3000 \text{ m} = 25.81 \text{ MPa} \qquad (6.2)$$

These values remain unchanged through the chapter. This assures that only the properties of the specific formation influence the calculations.

6.1 Sandstone

In sandstones, the WAB is primarily used for zonal isolation, and not as a barrier due to its permeability.

Formation properties:

Density	2.0 – 2.65 (2.325) s.g.
Young's modulus	0.1– 30 (15.05) GPa
Poisson's ratio	0 – 0.45 (0.225)
Biot's constant	1

First the overburden stress is calculated:

$$\sigma_v = -0.434 * 2.325 \ s.g.* 9843 \ ft = -9932 \ psi = -68.48 \ MPa \tag{6.3}$$

The horizontal stress in the formation is:

$$\sigma_h = -\left[\frac{0.225}{1-0.225}(68.48 \ MPa - 1 * 30.54 \ MPa) + 1 * 30.54 MPa\right]$$
$$= -41.55 \ MPa \tag{6.4}$$

The fracture pressure is:

$$p_{wf} = 2 * 41.55 \ MPa - 30.54 \ MPa = -52.57 \ MPa \tag{6.5}$$

This yields a maximum shrink pressure of:

$$p_{s,max} = -p_{wf} - p_f = 52.57 MPa - 25.81 \ MPa = 26.755 \ MPa \tag{6.6}$$

By solving the shrink pressure equation for Δu and inserting $p_{s,max}$, the maximum Δu is found:

$$\Delta u_{max} = p_{s,max}$$
$$* \left\{ \frac{c_o}{E_o(b^2 - c_o^2)}[(1 - v_o)c_o^2 + (1 + v_o)b^2] \right.$$
$$\left. + \frac{c_i}{E_i(c_i^2 - a^2)}[(1 - v_i)c_i^2 + (1 + v_i)a^2] \right\} \tag{6.7}$$

$$\Delta u_{max} = 0.594 \ mm$$

Now the previous results are compared to Figure 12 to see in which damage region the overpressure falls.

Convert the pressures to specific gravity:

$$p_w = \frac{25.81 * 10 \; bar}{0.0981 * 3000 \; m} = 0.877 \; s.g. \tag{6.8}$$

$$p_{s,max} = 0.909 \; s.g. \tag{6.9}$$

$$p_p = -1.038 \; s.g. \tag{6.10}$$

Total overpressure is:

$$p_o = p_w + p_{s,max} + p_p = 0.877 + 0.909 - 1.038 = 0.748 \; s.g. \tag{6.11}$$

By looking at Figure 12 it is seen that this pressure is in the plastic deformation region and causes crack initiation, but not fracture failure. The pressure where fracture is initiated is almost 0.8 s.g. This happens at a shrink pressure of:

$$p_{s,frac} = p_{s,max} + p_{frac} - p_o = 0.909 + 0.8 - 0.748 = 0.961 \; s.g. \tag{6.12}$$

$$p_{s,frac} = \frac{0.0981 * 3000 \; m * 0.961}{10 \; bar} = 28.28 \; MPa \tag{6.13}$$

which returns a Δu_{frac} of 0.627 mm.

From Figure 12 one can see that crack initiation starts at an overbalance of 0.5 s.g. the corresponding shrink pressure will then be:

$$p_{s.crack} = 0.877 + 0.5 - 1.038 = 0.339 \; s.g. = 9.98 \; MPa \tag{6.14}$$

This in turn gives a Δu_{crack} of 0.221 mm.

6.2   Shale

Since shales are non-permeable, it is ideal to place the WAB in these types of formations as a barrier.

Formation properties:

Density (s.g.)	2.3 – 2.8 (2.55)
Young's modulus (GPa)	0.4 – 70 (35.2)
Poisson's ratio	0 – 0.3 (0.15)
Biot's constant	1

Overburden stress:

$$\sigma_v = -75.10 \ MPa \tag{6.15}$$

Horizontal stress:

$$\sigma_h = -38.40 \ MPa \tag{6.16}$$

Fracture pressure:

$$p_{wf} = -46.27 \ MPa \tag{6.17}$$

Maximum shrink pressure:

$$p_{s,max} = 20.455 \ MPa = 0.695 \ s.g. \tag{6.18}$$

Which yields:

$$\Delta u_{max} = 0.298 \ mm \tag{6.19}$$

For this case, the total overpressure is:

$$p_o = 0.877 + 0.695 - 1.038 = 0.534 \ s.g. \tag{6.20}$$

This is barely exceeding the crack initiation pressure. Fracturing of the formation will occur at:

$$p_{s,frac} = 0.695 + 0.8 - 0.534 = 0.961 \ s.g. = 28.02 \ MPa \tag{6.21}$$

A fracture pressure of 28.02 MPa yields a Δu_{frac} of 0.621 mm.

6.3   High Porosity Chalk

Formation properties:

Density (s.g.)	1.4 – 1.7 (1.55)
Young's modulus (GPa)	0.5 – 5 (2.75)
Poisson's ratio	0.05 – 0.35 (0.1775)
Biot's constant	1

Overburden stress:

$$\sigma_v = -45.65 \ MPa \tag{6.22}$$

Horizontal stress:

$$\sigma_h = -33.80 \ MPa \tag{6.23}$$

Fracture pressure:

$$p_{wf} = -37.06 \ MPa \tag{6.24}$$

Maximum shrink pressure:

$$p_{s,max} = 11.249 \ MPa = 0.382 \ s.g. \tag{6.25}$$

Which yields:

$$\Delta u_{max} = 0.856 \ mm \tag{6.26}$$

Total overpressure is:

$$p_o = 0.877 + 0.382 - 1.038 = 0.221 \ s.g. \tag{6.27}$$

This is well within the stable wellbore region. Fracture of the formation will occur at:

$$p_{s,frac} = 0.382 + 0.8 - 0.221 = 0.961 \ s.g. = 28.28 \ MPa \tag{6.28}$$

The value of Δu_{frac} in this case will be 2.15 mm.

6.4   Low Porosity Chalk

Formation properties:

Density (s.g.)	1.7 – 2.0 (1.85)
Young's modulus (GPa)	5 – 30 (17.5)
Poisson's ratio	0.05 – 0.30 (0.175)
Biot's constant	1

Overburden stress:

$$\sigma_v = -54.49 \ MPa \tag{6.29}$$

Horizontal stress:

$$\sigma_h = -35.62 \ MPa \tag{6.306}$$

Fracture pressure:

$$p_{wf} = -40.70 \ MPa \tag{6.31}$$

Maximum shrink pressure:

$$p_{s,max} = 14.886 \ MPa = 0.506 \ s.g. \tag{6.32}$$

Which yields:

$$\Delta u_{max} = 0.297 \ mm \tag{6.33}$$

Total overpressure is:

$$p_o = 0.877 + 0.506 - 1.038 = 0.345 \ s.g. \tag{6.34}$$

This is well within the stable wellbore region. Fracturing of the formation will occur at:

$$p_{s,frac} = 0.506 + 0.8 - 0.345 = 0.961 \ s.g. = 28.02 \ MPa \tag{6.35}$$

The value of Δu_{frac} in this case will be 0.559 mm.

6.5   HPHT – Sandstone Case

Consider the sandstone case once again, but this time with a higher pore pressure causing it to be a HPHT well. The only thing that changes from the sandstone case is the pore pressure gradient, which is given a value of 0.9 psi/ft.

The pore pressure at the 3000 m depth is:

$$p_p = -61.01 \, MPa = 2.073 \, s.g. \tag{6.36}$$

Overburden stress:

$$\sigma_v = -68.48 \, MPa \tag{6.37}$$

Horizontal stress:

$$\sigma_h = -63.22 \, MPa \tag{6.38}$$

Fracture pressure:

$$p_{wf} = -65.37 \, MPa \tag{6.39}$$

Maximum shrink pressure:

$$p_{s,max} = 39.56 \, MPa = 1.344 \, s.g. \tag{6.40}$$

Which yields:

$$\Delta u_{max} = 0.878 \, mm \tag{6.41}$$

This is higher than the original case, which is caused by a larger horizontal stress that counteracts the pressure from the WAB.

The pore pressure is outside of the graph in Figure 12, and a fracturing pressure is therefore not calculated.

A high fracturing pressure will be beneficial in a HPHT well, as there are higher well pressures that need to be considered. This will most likely create a need for higher sealing pressures.

6.6 Summary

Important formation parameters:

- Density
  A higher formation density causes an increase in overburden and horizontal stress. This will in turn create higher fracture pressures, which allows for higher contact stresses and increased sealing potential.

- Pore pressure
  A higher pore pressure will increase the horizontal stress, but reduce the effective stress of the system. Ultimately, an increase in pore pressure will increase the fracture pressure due to the increase in horizontal stress being larger than the effective stress reduction.

- Poisson's ratio
  Horizontal stress increases with an increase in Poisson's ratio. This can cause a quite large fracture pressure, depending on the magnitude of the ratio.

- Young's modulus
  Changing the Young's modulus will not influence the fracturing pressure, but a low elasticity (high Young's modulus) means that the wellbore deformations will be smaller before fracturing occurs.

Taking these observations and results into consideration, it seems that an ideal placement for the WAB would be in a dense HPHT formation, with a high Poisson's ratio and Young's modulus. This will make sure that the formation can withstand high pressures, but at the same time experience as small deformations as possible.

The best placement of the WAB would then be in either sandstones or shales. Sandstones will be able to withstand a higher pressure, but will experience larger deformations compared to shales.

7. Effects of WAB and Formation Properties

In this chapter, the independent effects of the WAB and formation properties will be studied and explained.

Changes in the WAB properties will only influence the shrink pressure, but other stresses and pressures are included to give a broader picture of the situation. Formation properties can affect both formation pressure/stresses and shrink pressure.

7.1 Base Case

The sandstone example from the previous section is chosen as a base case. In this way, there are specific values to compare the results with.

WAB properties:

Outer radius	0.156 m
Thickness	0.012 m
Young's modulus	$200*10^3$ MPa
Poisson's ratio	0.3

Formation properties:

Outer radius	10000 m
Inner radius	0.1556 m
Young's modulus	$15.05*10^3$ MPa
Poisson's ratio	0.225
Biot's constant	1
Specific gravity	2.325 s.g.
Pore pressure	-10 MPa/km / -0.45 psi/ft
Depth	3000 m / 9843 ft.
Well fluid density	877 kg/m^3

These values yield the following results:

Shrink pressure (MPa)	18.021
Well pressure (MPa):	25.811
Pore pressure (MPa):	-30.538
Overburden stress (MPa):	-68.476
Horizontal stress (MPa):	-41.552
Fracture pressure (MPa):	-52.566

The radial deformations will be:

u_o (mm)	0.228
u_i (mm)	-0.172
c_{final} (m)	0.15583

The fracture pressure allows for a maximum shrink pressure and corresponding maximum wellbore radial deformation of:

Max shrink pressure (MPa):	26.755
Max Δu (mm)	0.594

Since the contact stress is equal to $\sigma_r = p_s$, the maximum shrink pressure is converted to compare the maximum allowable contact stress with the stress needed for sealing:

Max radial stress (psi)	3881

This is more than 15 times larger than what is necessary to create a seal.

7.2 Change in WAB Properties

7.2.1 Change in Outer Radius

One can easily see from the shrink pressure equation that an increase in Δu will increase the shrink pressure and vice versa. However, it is of interest to see in how large degree a change in the outer radius will affect the resulting shrink pressure.

An increase of 0.001 m is used, which gives a new outer radius of 0.157 m.

	Original	Increase
Shrink pressure (MPa):	18.021	62.715
Well pressure (MPa):	25.811	25.811
Pore pressure (MPa):	-30.538	-30.538
Overburden stress(MPa):	-68.476	-68.476
Horizontal stress (MPa):	-41.552	-41.552
Fracture pressure (MPa):	-52.566	-52.566
u_o (mm):	0.228	0.794
u_i (mm):	-0.172	-0.606
c_{final} (mm):	0.15583	0.15639
Max shrink pressure (MPa):	26.755	26.755
Max radial stress (psi):	3881	3881
Max Δu (mm)	0.594	0.597

The obvious, and only, effect an increase in outer diameter (larger Δu) has, is an increase in the shrink pressure. Even a small increase of just 1 mm has a significant effect, more than tripling the shrink pressure. This is obviously due a larger wellbore deformation.

A decrease in the outer radius will not be included as the results are obvious.

7.2.2 Change in Thickness
The thickness of the sleeve will also influence the shrink pressure to some degree.

New thicknesses of 25 mm and 8 mm are used, compared to 12 mm:

	Original	Increase	Decrease
Shrink pressure (MPa):	18.021	23.610	14.673
Well pressure (MPa):	25.811	25.811	25.811
Pore pressure (MPa):	-30.538	-30.538	-30.538
Overburden stress(MPa):	-68.476	-68.476	-68.476
Horizontal stress (MPa):	-41.552	-41.552	-41.552
Fracture pressure (MPa):	-52.566	-52.566	-52.566
u_o (mm):	0.228	0.299	0.186
u_i (mm):	-0.172	-0.101	-0.214
c_{final} (mm):	0.15583	0.15590	0.15579
Max shrink pressure (MPa):	26.755	26.755	26.755
Max radial stress (psi):	3881	3881	3881
Max Δu (mm)	0.594	0.453	0.729

As can be seen, a change in the thickness has some effect one the shrink pressure. The thicker the sleeve is, the higher the pressure will be. This is because a thicker sleeve causes a larger expansion into the formation. It also prevents more deformation.

7.2.3 Change in Young's Modulus

Different metals can be used on the WAB, and therefore provide a different Young's modulus. Steels usually take a value of 180 to 200 GPa. [20]

New Young's moduli of 220 and 180 GPa are used, compared to 200 GPa:

	Original	Increase	Decrease
Shrink pressure (MPa):	18.021	18.753	17.200
Well pressure (MPa):	25.811	25.811	25.811
Pore pressure (MPa):	-30.538	-30.538	-30.538
Overburden stress(MPa):	-68.476	-68.476	-68.476
Horizontal stress (MPa):	-41.552	-41.552	-41.552
Fracture pressure (MPa):	-52.566	-52.566	-52.566
u_o (mm):	0.228	0.238	0.218
u_i (mm):	-0.172	-0,162	-0.182
c_{final} (mm):	0.15583	0.15584	0.15582
Max shrink pressure (MPa):	26.755	26.755	26.755
Max radial stress (psi):	3881	3881	3881
Max Δu (mm)	0.594	0.571	0.622

Even though Δu is the same, the displacement will be different for both cylinders. Increasing the Young's modulus will let the WAB expand further into the formation, causing a larger shrink pressure.

7.2.4 Change in Poisson's Ratio

Most steels have a Poisson's ratio close to 0.3 It might still of interest to see how large effect a variation will have.

New Poisson's ratios of 0.305 (stainless steel) and 0.265 (steel, cast) [21] are used, compared to 0.3:

	Original	Increase	Decrease
Shrink pressure (MPa):	18.021	18.024	17.999
Well pressure (MPa):	25.811	25.811	25.811
Pore pressure (MPa):	-30.538	-30.538	-30.538
Overburden stress(MPa):	-68.476	-68.476	-68.476
Horizontal stress (MPa):	-41.552	-41.552	-41.552
Fracture pressure (MPa):	-52.566	-52.566	-52.566
u_o (mm):	0.228	0.228	0.228
u_i (mm):	-0.172	-0.172	-0.172
c_{final} (mm):	0.15583	0.15583	0.15583
Max shrink pressure (MPa):	26.755	26.755	26.755
Max radial stress (psi):	3881	3881	3881
Max Δu (mm)	0.594	0.594	0.595

These results show that a change in the Poisson's ratio of the WAB practically makes no difference. An increase will only cause a tiny increase in the shrink pressure, due to a larger expansion into the formation. A decrease allows for a slightly larger deformation.

7.2.5 Summary

A brief summary of the effects of the various WAB properties are:

- Increasing Δu will create a larger shrink pressure
- Increasing the sleeve thickness will create a larger shrink pressure due to larger expansion into the formation
- Increasing the Young's modulus will create a larger shrink pressure due to larger expansion into the formation
- A change in the Poisson's ratio will not have a significant effect (as long as it has a realistic value for steel)

7.3 Change in Formation Properties

Different formation parameter values have already been presented to some degree in the previous section, but here their independent effects will be studied more closely.

7.3.1 Change in Outer Radius

The outer radius of the formation will approach an infinite value. It is therefore interesting to see if the stresses and pressures will converge towards a value.

An outer radius of 100000 meters is used.

	Original	Increase
Shrink pressure (MPa):	18.021	18.021
Well pressure (MPa):	25.811	25.811
Pore pressure (MPa):	-30.538	-30.538
Overburden stress(MPa):	-68.476	-68.476
Horizontal stress (MPa):	-41.552	-41.552
Fracture pressure (MPa):	-52.566	-52.566
u_o (mm):	0.228	0.228
u_i (mm):	-0.172	-0.172
c_{final} (mm):	0.15583	0.15583
Max shrink pressure (MPa):	26.755	26.755
Max radial stress (psi):	3881	3881
Max Δu (mm)	0.594	0.594

There is no change in any of the results, which insinuates that the results converge towards a value. A decrease in the outer radius is not of relevance.
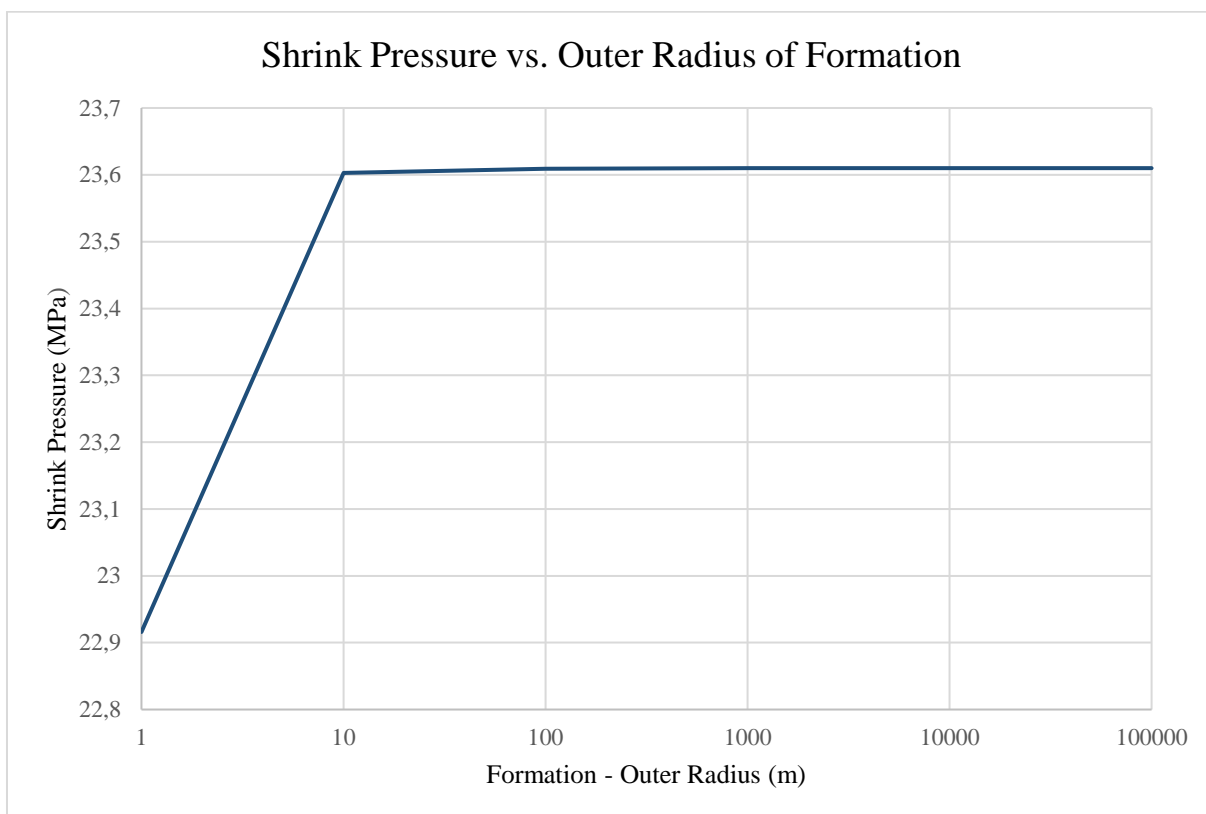
Figure 13: Shrink pressure vs. outer radius of formation

7.3.2 Change in Inner Radius

For curiosities sake, a change in the inner radius is considered as well to see if the results match with a change in the outer radius of the WAB. An inner radius that is larger than the outer radius of the WAB is not of interest (and will give a meaningless result), but giving it a value slightly smaller than the WAB should produce a smaller shrink pressure.

New inner radiuses of 0.1559 mm and 0.154 mm are used, compared to 0.1556 mm:

	Original	Increase	Decrease
Shrink pressure (MPa):	18.021	4.500	90.635
Well pressure (MPa):	25.811	25.811	25.811
Pore pressure (MPa):	-30.538	-30.538	-30.538
Overburden stress(MPa):	-68.476	-68.476	-68.476
Horizontal stress (MPa):	-41.552	-41.552	-41.552
Fracture pressure (MPa):	-52.566	-52.566	-52.566
u_o (mm):	0.228	0.057	1.136
u_i (mm):	-0.172	-0.043	-0.864
c_{final} (mm):	0.15583	0.15596	0.15514
Max shrink pressure (MPa):	26.755	26.755	26.755
Max radial stress (psi):	3881	3881	3881
Max Δu (mm)	0.594	0.595	0.590

The results are as expected, and fit the results from 7.2.1. A smaller outer radius causes a larger wellbore deformation and thus a higher shrink pressure.

7.3.3 Change in Young's Modulus

As can be seen from the cases with various formations, the Young's modulus can vary greatly. Depending on the rock it can be anywhere in the range from 1.2 – 99.4 GPa. [4]

New values of 50 GPa and 1 GPa are used, compared to 15.05 GPa:

	Original	Increase	Decrease
Shrink pressure (MPa):	18.021	29.976	1.999
Well pressure (MPa):	25.811	25.811	25.811
Pore pressure (MPa):	-30.538	-30.538	-30.538
Overburden stress(MPa):	-68.476	-68.476	-68.476
Horizontal stress (MPa):	-41.552	-41.552	-41.552
Fracture pressure (MPa):	-52.566	-52.566	-52.566
u_o (mm):	0.228	0.114	0.095
u_i (mm):	-0.172	-0.286	-0.005
c_{final} (mm):	0.15583	0.15571	0.15600
Max shrink pressure (MPa):	26.755	26.755	26.755
Max radial stress (psi):	3881	3881	3881
Max Δu (mm)	0.594	0.357	5.355

An increase in Young's modulus increases the shrink pressure in this case as well. This is because the formation will not expand as much, resulting in a little smaller common radius.

Also note how large the difference in maximum Δu is in the case with the low Young's modulus compared to the case with the high Young's modulus. This is because a low modulus of elasticity means the formation can experience more elastic deformation before fracture occurs.

7.3.4 Change in Poisson's Ratio

Depending on the rock type, the Poisson's ratio can be anywhere in the range from 0-0.45. [12]

New values of 0.45 and 0.05 are used, compared to 0.225:

	Original	Increase	Decrease
Shrink pressure (MPa):	18.021	16.311	19.620
Well pressure (MPa):	25.811	25.811	25.811
Pore pressure (MPa):	-30.538	-30.538	-30.538
Overburden stress(MPa):	-68.476	-68.476	-68.476
Horizontal stress (MPa):	-41.552	-61.578	-32.534
Fracture pressure (MPa):	-52.566	-92.618	-34.531
u_o (mm):	0.228	0.245	0.213
u_i (mm):	-0.172	-0.155	-0.187
c_{final} (mm):	0.15583	0.15584	0.15581
Max shrink pressure (MPa):	26.755	66.807	8.720
Max radial stress (psi):	3881	3881	1265
Max Δu (mm)	0.594	1.638	0.178

These results show that the Poisson's ratio has a significant effect on the wellbore pressures and deformations. A large Poisson's ratio causes the formation to expand more and thus creating a lower shrink pressure and a higher allowable shrink pressure and Δu.

Notice also how it causes a larger horizontal stress, which again leads to a larger fracture pressure.

7.3.5 Change in Average Bulk Density

Formation densities can vary from 1.4-3.2 s.g. Varying densities will not affect the shrink pressure, but formation stresses/pressures will be.

New densities of 2.8 s.g. (shale) and 1.4 s.g. (high porosity chalk) [12] is used, compared to 2.325 s.g.:

	Original	Increase	Decrease
Shrink pressure (MPa):	18.021	18.021	18.021
Well pressure (MPa):	25.811	25.811	25.811
Pore pressure (MPa):	-30.538	-30.538	-30.538
Overburden stress(MPa):	-68.476	-82.465	-41.233
Horizontal stress (MPa):	-41.552	-45.613	-33.643
Fracture pressure (MPa):	-52.566	-60.689	-36.748
u_o (mm):	0.228	0.228	0.228
u_i (mm):	-0.172	-0.172	-0.172
c_{final} (mm):	0.15583	0.15583	0.15583
Max shrink pressure (MPa):	26.755	34.878	10.963
Max radial stress (psi):	3881	5059	1586
Max Δu (mm)	0.594	0.774	0.243

A higher density creates a higher overburden stress, which again creates a higher horizontal stress. This leads to a higher fracture pressure, higher Δu and higher maximum shrink pressure.

7.3.6 Increase in Pore Pressure Gradient

Pore pressures can vary, but it will not be lower than what is used in the base case. Only an increase is therefore considered. This was also partly looked at in the previous chapter in the HPHT case.

A new pore pressure gradient of -0.6 psi/ft is used, compared to -0.45 psi/ft:

	Original	Increase
Shrink pressure (MPa):	18.021	18.021
Well pressure (MPa):	25.811	25.811
Pore pressure (MPa):	-30.538	-40.717
Overburden stress(MPa):	-68.476	-68.476
Horizontal stress (MPa):	-41.552	-48.776
Fracture pressure (MPa):	-52.566	-56.835
u_o (mm):	0.228	0.228
u_i (mm):	-0.172	-0.172
c_{final} (mm):	0.15583	0.15583
Max shrink pressure (MPa):	26.755	31.024
Max radial stress (psi):	3881	4500
Max Δu (mm)	0.594	0.689

A high pore pressure gradient causes a larger horizontal stress. This causes an increase in the fracture pressure, but not so large since the pore pressure is also subtracted in the fracture pressure equation.

7.3.7 Change in Well Depth

It is interesting to see the effect of the placement of the WAB, as it will be used in several sections of the well.

New depths of 1200 ft. (3658 m) and 6000 ft. (1829 m) are used, compared to 9843 ft. (10000 m):

	Original	Increase	Decrease
Shrink pressure (MPa):	18.021	18.021	18.021
Well pressure (MPa):	25.811	31.468	15.734
Pore pressure (MPa):	-30.538	-37.230	-18.615
Overburden stress(MPa):	-68.476	-83.482	-41.741
Horizontal stress (MPa):	-41.552	-50.658	-25.329
Fracture pressure (MPa):	-52.566	-64.086	-32.043
u_o (mm):	0.228	0.228	0.228
u_i (mm):	-0.172	-0.172	-0.172
c_{final} (mm):	0.15583	0.15583	0.15583
Max shrink pressure (MPa):	26.755	32.618	16.309
Max radial stress (psi):	3881	4731	2366
Max Δu (mm)	0.594	0.724	0.362

This shows that all pressures and stresses, except for the shrink pressure, are effected and increase with depth. This means that the maximum allowable shrink pressure and deformation also increases with depth.

7.3.8 Change in Well Fluid Density

Pressures in the well can vary greatly depending on the fluid present.

New values of 1200 kg/m^3 (drilling fluid) and 790 kg/m^3 is used (crude oil, 48º API) [22] are used, compared to 877 kg/m^3:

	Original	Increase	Decrease
Shrink pressure (MPa):	18.021	18.021	18.021
Well pressure (MPa):	25.811	35.318	23.251
Pore pressure (MPa):	-30.538	-30.538	-30.538
Overburden stress(MPa):	-68.476	-68.476	-68.476
Horizontal stress (MPa):	-41.552	-41.552	-41.552
Fracture pressure (MPa):	-52.566	-52.566	-52.566
u_o (mm):	0.228	0.228	0.228
u_i (mm):	-0.172	-0.172	-0.172
c_{final} (mm):	0.15583	0.15583	0,15583
Max shrink pressure (MPa):	26.755	17.249	29.315
Max radial stress (psi):	3881	2502	4252
Max Δu (mm)	0.594	0.383	0.651

A low density will be beneficial, as it creates a larger pressure margin for the WAB. There is no change in the deformations.

7.3.9 Change in Biot's Constant

The Biot's constant can by definition not be larger than 1, so only a decrease is considered.

A partially saturated rock has a value between 0 and 1, 0.5 is used:

	Original	Decrease
Shrink pressure (MPa):	18.021	18.021
Well pressure (MPa):	25.811	25.811
Pore pressure (MPa):	-30.538	-30.538
Overburden stress(MPa):	-68.476	-68.476
Horizontal stress (MPa):	-41.552	-30.716
Fracture pressure (MPa):	-52.566	-30.894
u_o (mm):	0.228	0.228
u_i (mm):	-0.172	-0.172
c_{final} (mm):	0.15583	0.15583
Max shrink pressure (MPa):	26.755	5.083
Max radial stress (psi):	3881	737
Max Δu (mm)	0.594	0.113

The Biot's constant affects the horizontal stress. A lower value will create a lower horizontal stress, and therefore a lower fracture pressure. This means that the maximum allowable shrink pressure and deformations also decrease.

7.3.10 Summary

A brief summary of the effects of the various formation properties are:

- Increasing the outer radius will at small values increase the shrink pressure, but it will eventually converge towards a value
- Increasing the inner radius of the formation will decrease the shrink pressure
- Increasing the Young's modulus will prevent the formation from expanding as much, creating a higher shrink pressure
- Increasing the Poisson's ratio allows for larger deformations of the wellbore, creating smaller shrink pressures
- Increasing the density makes the formation able to withstand greater pressures before fracturing
- Increasing the pore pressure causes a higher fracture pressure due to a larger horizontal stress
- Increasing the setting depth causes higher formation stresses and also a larger fracture pressure
- Increasing does not affect the fracture pressure, but creates a smaller pressure window for the WAB
- Decreasing the Biot's constant causes a lower horizontal stress and therefore a lower fracture pressure

8. Discussion

The results from the previous cases and examples show that very small volumetric deformations of the wellbore lead to crack initiation and eventually fracture. Some WAB and formation properties can have an advantageous effect on the shrink pressure created or the fracturing pressure.

However, the pressures and stresses created are quite large. During the expansion process, it might be that the shrink pressure never reaches such a high value. This will assure that integrity of the formation is preserved.

The sealing capability of the WAB can unfortunately not be presumed from the results of this thesis. It is interesting yet to see how large the contact stress from the metal elements is, which in the sandstone case was more than 3800 psi (more than 15 times as much as what is needed around the rubber sealing elements). This should leave quite a large operation margin for the main sealing components.

Other answers can still be drawn from the results. The possibility for high contact stresses promotes better sealing capabilities against the formation. This means that properties which allow for high shrink pressures are beneficial. These are:

- Placing the WAB in formations with a high Poisson's ratio
- Placing the WAB in formations with large overburden stresses
- Placing the WAB in formations with high pore pressures
- Placing the WAB as deep as possible
- Placing the WAB in formations with high Biot's constant
- Have a low density fluid in the well

By looking at Figure 12 and comparing the results from the various formation cases, it appears that the graph is mostly valid for sandstones. However, since the maximum allowable shrink pressure is so close to the fracture pressure on the graph, it gives confidence that the calculations and theory behind the work is correct, at least for sandstones.

Assuming isotropy might not be a disadvantage in this case. Taking the example of the Arkansas Sandstone, the fracturing pressure was lower for the isotropic case than the anisotropic case. If this is the case for all isotropic vs. anisotropic cases, the maximum allowable shrink pressure here gives a more conservative value. It is much better to underestimate the strength of the formation rather than overestimating it.

The calculated fracture pressure was also a little lower for the sandstone case, compared to Figure 12, which gives an additional safety margin.

It is not known how any formation damage will affect the sealing ability of the WAB. The fracture pressure is considered for the most part in this thesis, it might be that it should rather be the crack initiation pressure that should be used. A worst case scenario would be that damage to the wellbore allows for leak paths in the near wellbore formation behind the WAB. This would allow for communication of the annuli above and below the WAB.

9. Conclusion

The model shows that fracturing occurs at small wellbore deformations, but the accompanying pressures and stresses created before fracture occurs are still quite large. This means that there should be significant margins for creating pressures/stresses around the rubber elements to create a seal.

Some formation types will be better suited for placement of the WAB. It is also possible to make changes to the design (thickness) of the WAB and material choices, to make it more suitable for certain cases.

From this, it seems reasonable to conclude that the results show good potential and further investigations should be done.

10.   Future Work

To take full advantage of the work done in this thesis, experiments should be done to find the true Δu_{frac}. This can be done by applying loads to rock samples and measuring its deformation before fracturing.

Once this is known, work should be done to correlate the expansion pressure to the shrink pressure. The shear pin could then be designed to break at the expansion pressure that creates the maximum allowable contact stress (including a safety margin). In this way, the tool would be optimized to crate as high sealing pressures as possible.

References

1. Bårdsen, J. and Dagestad, V. 2016. Evolution of a Well Annular Barrier for Mitigation of SCP. Presented as the SPE Bergen One Day Seminar, Grieghallen, Bergen, Norway, 20 April. SPE-180020-MS. https://doi.org/10.2118/180020-MS

2. Drechsler, J. R. et al., 2013. Qualification and Field Trial of a Metal Expandable Well Annular Barrier. Presented at the SPE/IADC Drilling Conference, Amsterdam, The Netherlands, 5-7 March. SPE-163511-MS. https://doi.org/10.2118/163511-MS

3. Welltec Oilfield Services. 2014. In-Situ Hydroforming of an Annular Barrier in Oil Wells. Internal Presentation.

4. Welltec Oilfield Services. 2016. WMIT Rev 3 Nov 2016 Esbjerg. Internal Presentation.

5. Welltec Oilfield Services. 2017. Completion Solutions – Maximize Well Returns. Internal Presentation.

6. Jacinto, C.C. et al. World's First: Annular Barrier Installed in a Subsea, Deepwater Well without the Use of Cement. Presented at the Offshore Technology Conference, Rio de Janeiro, Brazil, 27-29 October. OTC-26122-MS. https://doi.org/10.4043/26122-MS

7. Well Completion Design

8. Wipertrip. wipertrip – External Casing Packers, http://www.wipertrip.com/cementing/miscellaneous/325-external-casing-packers.html (accessed 6 March 2017)

9. PetroWiki. Packers, http://petrowiki.org/Packers#Retrievable_hydraulic-set_single-string_packer (accessed 6 March 2017)

10. Krilov, Z. et al. 2000. Investigation of a Long-Term Cement Deterioration Under a High-Temperature, Sour Gas Downhole Environment. Presented at the SPE International Symposium on Formation Damage Control, Lafayette, Louisiana, 23-24 February. SPE-58771-MS. https://doi.org/10.2118/58771-MS

11. Aadnøy, B. S. and Looyeh, R. 2010. *Petroleum Rock Mechanics*, first edition. Oxford: Elsevier Inc.

12. Fjær, E. et al. *Petroleum Related Rock Mechanics*, second edition. Oxford: Elsevier Inc.

13. Cheatham, J.B. and Rice, U. 1984. Wellbore Stability. *Journal of Petroleum Technology* **36** (06). SPE-13340-PA. https://doi.org/10.2118/13340-PA

14. Mesfin, B. 2016. Grading, Tube stress and Failure analysis. Compendium, University of Stavanger, Stavanger, Norway.

15. Boresi, A. P. and Schmidt, R. J. The Thick-Wall Cylinder In *Advanced Mechanics of Materials*, sixth edition, Chap. 11, 389-422. Hoboken, John Wiley & Sons Inc.

16. Proto Manufacturing. Residual Stress Info, http://www.protoxrd.com/residual-stress-info.html (accessed 5 April 2017)

17. PetroWiki. Glossary:HPHT, http://petrowiki.org/Glossary:HPHT (accessed 11 June 2017)

18. Backers, T. 2004. Fracture toughness determination and micromechanics of rock under mode I and mode II loading. PhD thesis, University of Potsdam, Potsdam, Germany.
19. Ovwigho, E. K., 2010. Fracture Propagation Modeling. Master's thesis, Univeristy of Stavanger, Stavanger, Norway.
20. The Engineering Toolbox. Modulus of Elasticity or Young's Modulus – and Tensile Modulus for Common Materials, http://www.engineeringtoolbox.com/young-modulus-d_417.html (accessed 6 June 2017)
21. The Engineering Toolbox. Poisson's Ratio, http://www.engineeringtoolbox.com/poissons-ratio-d_1224.html (accessed 7 June 2017)
22. The Engineering Toolbox. Liquids and Densities, http://www.engineeringtoolbox.com/liquids-densities-d_743.html (accessed 7 June 2017)

Appendix A: Thick Wall Cylinder Derivation

(Taken from [14])

To derive the Lamé equation for a thick wall cylinder, four components are needed:

1. Equilibrium equation (Newton's law)
2. Compatibility relations (geometrical relationship)
3. Constitutive stress-strain-temperature relation (Hooke's law)
4. Appropriate boundary conditions

Equation of Equilibrium

By disregarding body forces, the equation of equilibrium is given as:

$$r \frac{d\sigma_r}{dr} = \sigma_\theta - \sigma_r \qquad \text{(A1)}$$

Strain-Displacement Relations

There are three strain-displacement relations for extensional strains:

$$\varepsilon_r = \frac{\partial u}{\partial r} \qquad \text{(A2)}$$

$$\varepsilon_\theta = \frac{u}{r} \qquad \text{(A3)}$$

$$\varepsilon_z = \frac{\partial w}{\partial z} \qquad \text{(A4)}$$

Where $u = u(r, z)$ and $w = w(r, z)$ denote components in the r and z directions, respectively.

If there is radial symmetry and ε_z is constant, eq. A2 and A3 becomes:

$$r \frac{d\varepsilon_\theta}{dr} = \varepsilon_r - \varepsilon_\theta \qquad \text{(A5)}$$

Which is the strain compatibility condition for a thick-walled cylinder.

Stress-Strain-Temperature Relations

For a cylinder that is made up of an isotropic and linearly elastic material, the stress-strain-temperature relations are given as:

$$\varepsilon_{rr} = \frac{1}{E}[\sigma_{rr} - v(\sigma_{\theta\theta} + \sigma_{zz})] + \alpha\Delta T \tag{A6}$$

$$\varepsilon_{\theta\theta} = \frac{1}{E}[\sigma_{\theta\theta} - v(\sigma_{rr} + \sigma_{zz})] + \alpha\Delta T \tag{A7}$$

$$\varepsilon_{zz} = \frac{1}{E}[\sigma_{zz} - v(\sigma_{rr} + \sigma_{\theta\theta})] + \alpha\Delta T \tag{A8}$$

Boundary Conditions

For a cylinder that is exposed to both external and internal pressures, the boundary conditions are:

$$(\sigma_r)_{r=a} = -p_a \tag{A9}$$

$$(\sigma_r)_{r=b} = -p_b \tag{A10}$$

In this case, the negative integer signifies a compressive stress.

Development of the Stress Component Expressions

Assume a plane strain condition and reformulate eqs. A6-A8:

$$\sigma_r - v(\sigma_\theta + \sigma_z) = E\varepsilon_r - E\alpha\Delta T \tag{A11}$$
$$\sigma_\theta - v(\sigma_r + \sigma_z) = E\varepsilon_\theta - E\alpha\Delta T \tag{A12}$$
$$\sigma_z - v(\sigma_r + \sigma_\theta) = -E\alpha\Delta T \tag{A13}$$

Solve eq. A13 for σ_z and insert in eq. A6 and A7:

$$\sigma_r - v[\sigma_\theta + v(\sigma_r + \sigma_\theta) - E\alpha\Delta T] = E\varepsilon_r - E\alpha\Delta T \tag{A14}$$
$$\sigma_\theta - v[\sigma_r + v(\sigma_r + \sigma_\theta) - E\alpha\Delta T] = E\varepsilon_\theta - E\alpha\Delta T \tag{A15}$$

Expanding and then simplifying eqs. A14 and A15 yields:

$$\sigma_r(1 - v^2) - v\sigma_\theta(1 + v) + vE\alpha\Delta T = E\varepsilon_r - E\alpha\Delta T \tag{A17}$$
$$\sigma_\theta(1 - v^2) - v\sigma_r(1 + v) + vE\alpha\Delta T = E\varepsilon_\theta - E\alpha\Delta T \tag{A18}$$

The next step is to multiply eq. A17 by *(1-v)* and eq. A18 with *v* and then adding them together:

$$\sigma_r(1 - v^2)(1 - v) - v^2\sigma_r(1 + v)$$
$$= (1 - v)E\varepsilon_r - (1 - v)E\alpha\Delta T + vE\varepsilon_\theta - vE\alpha\Delta T$$
$$- (1 - v)vE\alpha\Delta T - v^2E\alpha\Delta T$$

(A19)

Simplification of eq. A19 leads to:

$$\sigma_r(1 + v)(1 - 2v) = E[(1 - v)\varepsilon_r + v\varepsilon_\theta] - (1 + v)E\alpha\Delta T$$

(A20)

Which finally gives the radial stress:

$$\sigma_r = \frac{E}{(1 + v)(1 - 2v)}[(1 - v)\varepsilon_r + v\varepsilon_\theta] - \frac{E\alpha\Delta T}{1 - 2v}$$

(A21)

A similar process is done to solve for σ_z and σ_θ:

$$\sigma_\theta = \frac{E}{(1 + v)(1 - 2v)}[v\varepsilon_r + (1 - v)\varepsilon_\theta] - \frac{E\alpha\Delta T}{1 - 2v}$$

(A22)

$$\sigma_z = \frac{E}{(1 + v)(1 - 2v)}v[\varepsilon_r + \varepsilon_\theta] - \frac{E\alpha\Delta T}{1 - 2v}$$

(A23)

Then insert the strain-displacement relation:

$$\sigma_r = \frac{E}{(1 + v)(1 - 2v)}\left[v\frac{u}{r} + (1 - v)\frac{\partial u}{\partial r}\right] - \frac{E\alpha\Delta T}{1 - 2v}$$

(A25)

$$\sigma_\theta = \frac{E}{(1 + v)(1 - 2v)}\left[v\frac{\partial u}{\partial r} + (1 - v)\frac{u}{r}\right] - \frac{E\alpha\Delta T}{1 - 2v}$$

(A26)

Substitute the radial and hoop stress expressions into the equation of equilibrium to obtain:

$$\frac{E(1 - v)}{(1 + v)(1 - 2v)}\left[\frac{\partial^2 u}{\partial r^2} + \frac{1}{r}\frac{\partial u}{\partial r} - \frac{u}{r^2}\right] - \frac{E\alpha}{1 - 2v}\frac{\partial \Delta T}{\partial r} + F_r = 0$$

(A27)

Have that:

$$\frac{\partial^2 u}{\partial r^2} + \frac{1}{r}\frac{\partial u}{\partial r} - \frac{u}{r^2} = \frac{\partial}{\partial r}\left[\frac{1}{r}\frac{\partial}{\partial r}(ru)\right] \tag{A28}$$

$$\frac{\partial}{\partial r}\left[\frac{1}{r}\frac{\partial}{\partial r}(ru)\right] = \frac{\alpha(1+v)}{1-v}\frac{\partial\Delta T}{\partial r} \tag{A29}$$

Body forces are ignored, as well as temperature effects:

$$\frac{\partial}{\partial r}\left[\frac{1}{r}\frac{\partial}{\partial r}(ru)\right] = 0 \tag{A30}$$

By integrating eq. 20, an expression for the displacement field u is found:

$$u = \frac{1}{2}C_1 r + \frac{C_2}{r} \tag{A31}$$

Where C_1 and C_2 are integration constants.

The hoop stress and radial stress expressions can then be reformulated:

$$\sigma_r = \frac{E}{(1+v)(1-2v)}\left[\frac{1}{2}C_1 - (1-2v)\frac{C_2}{r^2}\right] \tag{A32}$$

$$\sigma_\theta = \frac{E}{(1+v)(1-2v)}\left[\frac{1}{2}C_1 + (1-2v)\frac{C_2}{r^2}\right] \tag{A33}$$

$$\sigma_z = v(\sigma_\theta + \sigma_r) = \frac{Ev}{(1+v)(1-2v)}2C_1 \tag{A34}$$

Boundary conditions are applied to determine C_1 and C_2:

$$\frac{1}{2}C_1 - (1-2v)\frac{C_2}{a^2} = -\frac{(1+v)(1-2v)}{E}p_a \tag{A35}$$

$$\frac{1}{2}C_1 - (1-2v)\frac{C_2}{b^2} = -\frac{(1+v)(1-2v)}{E}p_b \tag{A36}$$

Solve for C_1 and C_2:

$$C_1 = \frac{(1+v)(1-2v)}{E}\frac{2(p_a a^2 - p_b b^2)}{b^2 - a^2} \tag{A37}$$

$$C_2 = \frac{1+v}{E} \frac{a^2 b^2 (p_a - p_b)}{b^2 - a^2} \tag{A38}$$

Finally, the stress component equations can be solved by substituting the constants:

$$\sigma_r = \frac{p_1 a^2 - p_2 b^2}{b^2 - a^2} - \frac{a^2 b^2}{r^2(b^2 - a^2)}(p_1 - p_2) \tag{A39}$$

$$\sigma_\theta = \frac{p_1 a^2 - p_2 b^2}{b^2 - a^2} + \frac{a^2 b^2}{r^2(b^2 - a^2)}(p_1 - p_2) \tag{A40}$$

$$\sigma_z = 2v \frac{p_1 a^2 - p_2 b^2}{b^2 - a^2} \tag{A41}$$

Appendix B: Psi – Pa Conversion

$$psi = {}^{lbf}\!/_{ft}$$ (B1)

$$Pa = {}^{N}\!/_{m^2}$$ (B2)

1 lb	4.448 N
1 $in.$	0.0254 m

$$1 \, {}^{lb}\!/_{in^2} * \left(\frac{1}{0.0254 \, {}^{in}\!/_{m}} \right)^2 * 4.448 \, {}^{N}\!/_{lb} = 6894.4 \, {}^{N}\!/_{m^2}$$ (B3)

$$1 \, psi = 6894.4 \, Pa$$ (B4)

$$1 \, Pa = \frac{1}{6894.4} psi = 1.45 * 10^{-4} psi$$ (B5)